
The Two-Stage Decision-Sampling Hypothesis: Understanding the Emergence of Self-Reflection in RL-Trained LLMs

Zibo Zhao[†]

Arizona State University
zzhao203@asu.edu

Yuanting Zha

ShanghaiTech University
zhayt2022@shanghaitech.edu.cn

Haipeng Zhang[§]

ShanghaiTech University
zhanghp@shanghaitech.edu.cn

Xingcheng Xu[§]

Shanghai Artificial Intelligence Laboratory
xingcheng.xu18@gmail.com

Abstract

Self-reflection capabilities emerge in Large Language Models after RL post-training, with multi-turn RL achieving substantial gains over SFT counterparts. Yet the mechanism of how a unified optimization objective gives rise to functionally distinct capabilities of generating solutions and evaluating when to revise them remains opaque. To address this question, we introduce the Gradient Attribution Property to characterize how reward gradients distribute across policy components, formalized through the Two-Stage Decision-Sampling (DS) Hypothesis, which decomposes the policy into sampling (π_{sample}) for generation and decision (π_d) for verification. We prove that surrogate rewards exhibit Balanced Gradient Attribution, while SFT and KL penalties exhibit Unbalanced Gradient Attribution, with length-weighting creating asymmetric regularization that constrains π_{sample} while leaving π_d under-optimized, providing a theoretical explanation of why RL succeeds where SFT fails. We also empirically validate our theoretical predictions on arithmetic reasoning demonstrates that RL’s superior generalization stems primarily from improved decision-making (π_d) rather than sampling capabilities, providing a first-principles mechanistic explanation for self-correction in thinking models.

1 Introduction

Self-reflection capabilities—the ability to verify reasoning, detect errors, and revise incorrect answers—emerge spontaneously in large language models after RL post-training (DeepSeek-AI et al., 2025; OpenAI et al., 2024; Bercovich et al., 2025; Zhao et al., 2024). This emergent behavior correlates strongly with substantial performance improvements, particularly in mathematical reasoning tasks where models trained with multi-turn RL achieve significant gains over their supervised fine-tuning (SFT) counterparts. Yet despite clear and widely documented performance improvements, the mechanism by which RL training produces these qualitatively different capabilities remains theoretically opaque: it is unclear how a unified reinforcement learning objective gives rise to functionally distinct multitasking abilities¹, and why RL succeeds at inducing this functional separation where SFT consistently fails.

A sharp contrast exists between training regimes: multi-turn RL algorithms, such as GRPO, successfully induce self-reflection where single-turn reinforcement learning and standard SFT consistently

¹The ability of generating candidate solutions and the ability of evaluating when to accept or revise them.

fail. While existing literature extensively records what occurs—the emergence of verification and revision behaviors—it lacks an anatomical explanation of how the training objective fundamentally alters the model’s policy to enable this. Specifically, it remains unclear how and which unified optimization processes drive the functional separation required for self-correction—distinguishing the capability to generate solutions from the capacity to evaluate them. To bridge this gap, we must look beyond surface-level performance and examine the underlying gradient dynamics that govern this behavioral bifurcation.

We view learning to self-reflect as a specification of learning to multitask with a shared policy function. Large language models perform multiple cognitive operations—generating content, evaluating quality, deciding whether to continue—through a single next-token prediction mechanism. Under this multitasking framework, we introduce the Gradient Attribution Property to characterize how reward gradients distribute across policy components. We formalize this through the Two-Stage Decision-Sampling (DS) Hypothesis, which conceptually decomposes the model’s unified policy into a sampling policy π_{sample} for content generation and a decision policy π_d for verification and stopping. Crucially, RL training can improve these two components symmetrically or asymmetrically depending on the reward structure. When a model develops self-reflection capabilities, it is primarily learning to improve the decision policy (π_d)—the model’s judgment about when to trust versus revise its outputs—rather than (or in addition to) improving its raw sampling capabilities (π_{sample}). This decomposition transforms the phenomenological observation of “emergent self-reflection” into a precise quantitative question about gradient flow: how does the RL objective differentially update these two policy components, and how does this differential updating determine what the model learns?

To answer this question, we develop the concept of gradient attribution property for analyzing how reward gradients are distributed between policy components. We prove that different reward structures induce fundamentally different learning dynamics. Surrogate rewards exhibit Balanced Gradient Attribution: variations in the reward signal map cleanly to variations in whichever policy component was actually responsible for the outcome, creating symmetric learning pressure on both π_{sample} and π_d . In contrast, KL-divergence penalties exhibit Unbalanced Gradient Attribution: the length-weighting inherent in token-level KL calculations creates asymmetric regularization that heavily constrains π_{sample} while leaving π_d relatively unconstrained. The Balanced Gradient Attribution property of surrogate reward explains why RL succeeds: the mathematical structure of its objective necessarily favors learning better π_d . Conversely, SFT resembles a KL-divergence like objective without the countervailing reward signal, explaining its systematic failure to develop genuine self-reflection as observed in the literature.

We make several contributions. First, we formalize the DS-Hypothesis with explicit policy decomposition and mathematically characterize when gradient signals can be cleanly attributed to specific policy component. Second, we provide a first-principles mechanistic account of why RL training algorithms like GRPO induce self-reflection capabilities while SFT does not, grounded in the gradient attribution properties of their respective objectives. Third, we empirically validate the framework’s predictive power by training models on arithmetic reasoning tasks and demonstrating that: (i) the framework accurately predicts model performance using calibrated π_{sample} and π_d parameters; (ii) RL training indeed improves π_d more than π_{sample} ; and (iii) generalization to out-of-distribution tasks is primarily limited by π_{sample} rather than π_d , as the framework predicts. Finally, we use the framework to explain documented empirical phenomena, including why SFT models exhibit the “echoing effect”² and why reflection-rich SFT data improves first-answer accuracy without enabling genuine self-correction.

The remainder of this paper proceeds as follows. Section 2 positions our work within three research streams: policy gradient methods for LLM training, mathematical reasoning and generalization in Transformers, and the evolution of self-correction from prompting to learned RL behaviors. Section 3 develops the theoretical framework, introducing the gradient attribution property and proving our main results for surrogate rewards and KL penalties. Section 4 presents empirical validation through experiments on arithmetic reasoning tasks, including calibration studies and tests of the framework’s predictions. Section 5 applies the theoretical insights to explain SFT’s limitations and compares

²Kang et al. (2025) found that SFT-trained thinking models never learn to discriminate between correct and incorrect answers; post-reflection answers largely echo pre-reflection ones.

SFT versus RL generalization patterns. Section 6 concludes with implications and future research directions.

2 Related Work

Our work lies at the intersection of three distinct research streams: the control-theoretic foundations of policy gradients, the mechanics of mathematical generalization in Transformers, and the evolution of self-correction from inference-time prompting to intrinsic reinforcement learning. While each stream has developed largely independently, we unify them through the Gradient Attribution Property framework. From policy gradient theory, we borrow the analytical tools for decomposing reward gradients; from the mathematical reasoning literature, we adopt arithmetic tasks as a controlled testbed where generalization can be precisely measured; from the self-correction literature, we take the empirical puzzle that motivates our theory—why RL induces genuine self-reflection where SFT produces only surface-level mimicry. Our contribution is to provide a mechanistic explanation that bridges these streams: the gradient attribution properties of different training objectives determine whether models learn genuine decision-making capabilities or merely imitate reflective text patterns. We review each stream in turn below, positioning our framework relative to existing theoretical and empirical foundations.

2.1 Foundations and Practices of Policy Optimization Methods

The transition from supervised imitation to reinforcement learning in reasoning models rests fundamentally on control theory of policy gradients. [Sutton et al. \(1999a\)](#) expanded the horizon of reinforcement learning by introducing *options*—temporally extended actions within a semi-Markov decision process (SMDP). This framework provides the essential theoretical justification for treating a multi-token “Chain of Thought” not merely as a sequence of predictions, but as sequences of optimizable moves. [Agarwal et al. \(2020\)](#) provides an excellent review of the theory as well as discussion on the convergence properties of these methods³. Policy gradient methods have long been empirically successful and have recently been widely applied in post-training LLMs ([Ouyang et al., 2022](#); [Stiennon et al., 2020](#)). Prominent algorithms include Trust Region Policy Optimization (TRPO)⁴ ([Schulman et al., 2017a](#)), Proximal Policy Optimization (PPO)⁵ ([Schulman et al., 2017b](#)), and Direct Preference Optimization (DPO) ([Rafailov et al., 2024](#)), among others. More recently, [Shao et al. \(2024\)](#) introduced Group Relative Policy Optimization (GRPO), which eliminates the need for value networks by normalizing rewards within group samples has been proved useful in post-training LLM to thinking models that demonstrated some emerging ability to do self-reflection ([DeepSeek-AI et al., 2025](#))⁶.

2.2 Mathematical Reasoning and Generalization

Arithmetic reasoning serves as a rigorous testbed for probing the limits of Transformer generalization. Early work by [Nogueira et al. \(2021\)](#) and [Anil et al. \(2022\)](#) established that standard Transformers, despite scale, exhibit catastrophic failures in length extrapolation (OOD), suggesting they learn surface heuristics rather than robust algorithms. [Lee et al. \(2023\)](#) challenged the necessity of scale, demonstrating that small models could master arithmetic via rigorous data formatting (e.g., scratchpads) and reverse-order generation, identifying sharp phase transitions in learning indicative of “grokking”. The underlying mechanics of these failures were formalized by [Xu et al. \(2025\)](#), who developed a unified theoretical framework linking generalization to the alignment between model architecture (specifically Relative Positional Encoding) and task symmetry (translational invariance). In more general settings beyond simple arithmetic operations, mathematical reasoning

³Our work here does not touch on the convergence properties of policy gradient methods; however, these convergence issues are the reason we limit our demonstration examples to a single dimension.

⁴Notable feature of TRPO: constrains policy updates using KL-divergence to ensure stable learning.

⁵PPO simplifies TRPO through a clipping mechanism while maintaining stability and has become the de facto standard for RLHF.

⁶In the theoretical sections of this paper, we do not consider clipping or trust-region constraints, which compromise the analytical tractability of the reward function in favor of practical training stability. Although GRPO is closest to our theoretical setting, we acknowledge that technical differences remain; our framework is an abstraction of policy-based algorithms rather than a formalization of any specific one.

also serves as a critical testing ground for measuring the reasoning ability of LLMs. Widely used benchmarks include GSM8K, MATH, and MetaMathQA, among others are widely used in measuring mathematical reasoning ability of LLMs (Cobbe et al., 2021; Hendrycks et al., 2021; Yu et al., 2024). More recently, these benchmarks have evolved toward greater comprehensiveness and higher difficulty levels (Tang et al., 2024; Phan et al., 2025). We adopt mathematical reasoning as our empirical context for its clarity in evaluating learning effects⁷.

2.3 RL-Reflection and Self-Correction

The capability for self-correction has evolved from prompt engineering to learned intrinsic behaviors. While Wei et al. (2022) and Feng et al. (2023) established the computational necessity of intermediate reasoning steps, critical surveys by Kamoi et al. (2024) and Huang et al. (2024) revealed that "intrinsic self-correction" in SFT models is often illusory or dependent on Oracle feedback. Recent advances have moved toward instilling genuine verification via Reinforcement Learning. Kumar et al. (2024) (SCoRe) identified the distribution mismatch in SFT-based correction—training on others' mistakes versus correcting one's own—and proposed multi-turn RL on self-generated traces as the solution. This trajectory has culminated in frameworks like Self-Rewarding Correction (Xiong et al., 2025) and Policy as Generative Verifier (PAG) (Jiang et al., 2025), which unify the "Solver" and "Critic" into a single policy. Most relevant to our work, Zhao et al. (2025) and Ma et al. (2025) explicitly break down policies into 'generating answer' and 'verification', demonstrating RL with explicit breakdown policies can yield higher performance in mathematical reasoning tasks. Notably, we focus on the 'implicit breakdown of policy functions' in this paper which drives the 'emergent self-reflection' ability in Deepseek-R1 like thinking models.

3 Formalization of The Decision-Sampling Hypothesis

We develop a formal framework to explain why RL post-training produces self-reflection capabilities. The key concept is the **gradient attribution property**, which characterizes how reward gradients distribute to its policy components. When a model performs multiple conceptually distinct functions through a single policy, rewards with Balanced Gradient Attribution enable effective learning to perform all functions, while rewards with imperfect attribution cause the model to learn some functions ineffectively. The decomposition into sub-policies is purely conceptual—with perfect attribution, training a unified policy is equivalent to training decomposed sub-policies with properly attributed rewards.

We model an LLM solving query Q as a sequential decision process. At each iteration $k \geq 1$, the model executes two operations:

- Sample a candidate answer A_k with internal reasoning T_k (the "thoughts")
- Decide whether to output this answer (STOP) or generate another attempt (RESAMPLE)

We prove that surrogate rewards⁸ and KL-penalties exhibit fundamentally different gradient attribution properties. This difference explains why SFT-trained thinking models lack genuine self-reflection: they perform better on first attempts, with self-reflective behavior providing little improvement in answer correctness.

Section 3.1 introduces our formal setting; Section 3.2 defines gradient attribution; Section 3.3 analyzes surrogate rewards and KL-penalties. Section 5 later applies these results to explain SFT behavior.

3.1 Settings and Preliminary

State Space The state at step k is $s_k = (Q, A_k, T_k)$, encoding the query and the model's current candidate solution.

Policy Decomposition The overall policy π_θ decomposes into two components:

⁷Ideally, our framework would apply to more general settings; however, developing valid measurements in other domains would be more challenging.

⁸In practice, RL training typically uses variations like the clipped surrogate reward for stability. We analyze the simple surrogate reward for its analytical tractability.

- Sampling policy $\pi_{\text{sample}}(\cdot|s_{k-1}; \theta)$: distribution over (A_k, T_k) given context
- Decision policy $\pi_d(\cdot|s_k; \theta)$: distribution over STOP, RESAMPLE given current state

Trajectory Probability Factorization: A trajectory τ of length T consists of a sequence of samples and decisions:

$$\tau = (A_1, T_1, \text{RESAMPLE}, A_2, T_2, \text{RESAMPLE}, \dots, A_T, T_T, \text{STOP})$$

Lemma 1. *The probability of trajectory τ under policy π_θ factorizes as:*

$$P(\tau|Q; \theta) = \left[\prod_{k=1}^T \pi_{\text{sample}}(A_k, T_k|s_{k-1}; \theta) \right] \cdot \left[\prod_{k=1}^{T-1} \pi_d(\text{RESAMPLE}|s_k; \theta) \right] \cdot \pi_d(\text{STOP}|s_T; \theta)$$

Corollary 1. *The log-probability gradient separates into sampling and decision components:*

$$\nabla_\theta \log P(\tau|Q; \theta) = \underbrace{\sum_{k=1}^T \nabla_\theta \log \pi_{\text{sample}}(A_k, T_k|s_{k-1}; \theta)}_{\text{sampling gradient}} + \underbrace{\sum_{k=0}^T \nabla_\theta \log \pi_d(a_k|s_k; \theta)}_{\text{decision gradient}}$$

where $a_k \in \text{RESAMPLE}, \text{STOP}$ denotes the decision at step k .

Reward Function For query Q with ground truth answer A_Q^* , the reward of trajectory τ ending at step T is:

$$R(\tau) = \mathbb{I}(A_T = A_Q^*)$$

Thus, for a given policy π_θ and reward function R , define:

$$Q_R^\pi(s, a) = \mathbb{E}_{\pi_\theta} \left[\sum_{k=t}^{\infty} \gamma^{k-t} R_k \mid s_t = s, a_t = a \right]$$

where $\gamma \in (0, 1]$ is the discount factor.

Lemma 2. *The gradient of the expected return decomposes as:*

$$\nabla_\theta J(\theta) = \mathbb{E}_{\tau \sim \pi_\theta} \left[\sum_{t=0}^T \left(\nabla_\theta \log \pi_{\text{sample}}(a'_t|s_{t-1}) \cdot Q_{\text{sample}}^\pi(s_{t-1}, a'_t) + \nabla_\theta \log \pi_d(a''_t|s_t) \cdot Q_d^\pi(s_t, a''_t) \right) \right]$$

where $a'_t = (A_t, T_t)$ denotes sampling actions and $a''_t \in \text{RESAMPLE}, \text{STOP}$ denotes decision actions.

Lemma 2 is a direct adaptation of the standard policy gradient theorem (Sutton et al., 1999b) to our factorized policy structure.

3.2 Gradient Attribution Property

We formalize gradient attribution through the information structure of Q-values.

Definition 3.1 (Gradient Attribution Property). Consider a reward function R and the induced Q-values $Q_{\text{sample}}^\pi(s, a')$ and $Q_d^\pi(s, a'')$ under policy π_θ .

A reward R exhibits **balanced gradient attribution** if the Q-values admit a decomposition:

$$Q_{\text{sample}}^\pi(s_{k-1}, a'_k) = f_{\text{sample}}(s_{k-1}, a'_k, \Phi(s_k))$$

$$Q_d^\pi(s_k, a''_k) = f_d(s_k, a''_k, \Phi(s_{k+1}))$$

where $\Phi: \mathcal{S} \rightarrow \mathbb{R}$ is a scale-invariant sufficient statistic and the weighting functions f_{sample}, f_d are of comparable magnitude: $f_{\text{sample}} = \Theta(f_d)$

A reward exhibits **unbalanced gradient attribution** if the Q-values decompose as:

$$Q_{\text{sample}}^\pi(s_{k-1}, a'_k) = r_k^{\text{sample}} + \gamma \cdot V^\pi(s_k)$$

$$Q_d^\pi(s_k, a''_k) = r_k^{\text{decision}} + \gamma \cdot V^\pi(s_{k+1})$$

where the immediate reward components satisfy $|r_k^{\text{sample}}| = \omega(|r_k^{\text{decision}}|)$ systematically (i.e., scale-separated by more than a constant factor across typical trajectories).

Interpretation: Perfect attribution means both Q -values can be expressed in terms of the same information about future rewards (the sufficient statistic Φ), just evaluated at different states along the trajectory. This allows the unified network to learn a consistent representation of "future value" that both π_{sample} and π_d can use.

Imperfect attribution means the Q -values require different information about the future (Φ_{sample} vs Φ_d). The unified network cannot learn a single coherent representation of future value—attempting to do so leads to "mismeshing" the gradient signals, where updates intended for one conceptual function interfere with learning the other.

Remark (perfect attribution). In the case of perfect attribution, we can identify $\Phi(s) = V^\pi(s)$ as the state value function. This is the standard Bellman decomposition:

$$Q^\pi(s, a) = \mathbb{E}[R(s, a) + \gamma V^\pi(s')|s, a]$$

The key is that the *same* V^π appears in the decomposition for both policy components.

Remark (When imperfect attribution arise?). Consider a reward structure where:

- The immediate reward for sampling depends on sequence length: $r_{\text{sample}} \sim O(L_k)$
- The immediate reward for decisions is scalar: $r_d \sim O(1)$
- Future value recursively depends on these asymmetric immediate rewards

Then Φ_{sample} must encode "accumulated future sampling costs" while Φ_d encodes "accumulated future decision costs", which are fundamentally different scales. This is precisely what happens with the KL penalty, as we show in the section 3.3.

Remark. Operational Identification of Decision Actions he decomposition into π_{sample} and π_d is an analytical abstraction—the model architecturally remains a single next-token predictor. However, decision actions can be operationalized through identifiable proxy tokens that signal verification or revision intent. In our experiments, we detect decision boundaries via lexical markers including "I'll go back and check", "Let me recompute", "I made a mistake" and similar verification phrases. The token sequence following such markers until the next candidate answer constitutes a decision action, while extended generation of reasoning and answers constitutes sampling actions. This operationalization enables the calibration reported in Section 4.2: we estimate $p_d|C$ and $p_d|W$ by observing stopping and resampling behavior conditional on answer correctness, where "resampling" is identified by the presence of revision markers followed by a new solution attempt

3.3 Gradient Attribution of Surrogate Reward and KL Penalty

In this subsection, we analyze the gradient attribution properties of two fundamental reward functions used in RLM training.

3.3.1 Simple Surrogate Reward Has Balanced Gradient Attribution

The simple surrogate reward with advantage A_i for trajectory τ_i is:

$$L_{\text{reward}}(\theta) = \mathbb{E}_{\tau_i \sim \pi_{\text{old}}} \left[\frac{\pi_\theta(\tau_i|Q_i)}{\pi_{\text{old}}(\tau_i|Q_i)} A_i \right]$$

where A_i is the group-relative advantage measuring whether trajectory τ_i is better or worse than the average trajectory for query Q_i .

Theorem 3.1. *For the surrogate reward objective with trajectory-level advantage A_i , the Q -values satisfy:*

$$Q_{\text{sample}}^{\pi, \text{reward}}(s_{k-1}, a'_k) = \gamma^{\sum_{j=k}^T \text{len}(A_j, T_j)} \cdot A_i$$

$$Q_d^{\pi, \text{reward}}(s_k, a''_k) = \gamma^{\sum_{j=k}^T \text{len}(A_j, T_j)} \cdot A_i$$

*The sufficient statistic $\Phi(s_k) = \gamma^{\sum_{j=k}^T \text{len}(A_j, T_j)} A_i$ is **scale-invariant**: it enters both Q -values as an identical multiplicative factor. Consequently, the advantage A_i weights gradient contributions to π_{sample} and π_d symmetrically.*

Proof Sketch. The advantage A_i is a trajectory-level scalar measuring overall quality. From the policy gradient theorem, the gradient is:

$$\nabla_{\theta} \mathcal{L}_{\text{reward}} = \mathbb{E}_{\tau_i} \left[A_i \sum_{k=1}^T \nabla_{\theta} \log \pi_{\text{sample}}(\cdot) + A_i \sum_{k=0}^T \nabla_{\theta} \log \pi_d(\cdot) \right]$$

The advantage multiplies both gradient components equally. Since both π_{sample} and π_d contributed to producing the trajectory that received advantage A_i , and the advantage reflects the *coupled* outcome (correct answer + appropriate stopping), both Q-values equal the length-discounted advantage. The key observation is that the advantage A_i is a trajectory-level scalar that does not decompose into action-specific components. From the policy gradient theorem: $\nabla_{\theta} \mathcal{L}_{\text{reward}} = \mathbb{E}_{\tau_i} [A_i \sum_{k=1}^T \nabla_{\theta} \log \pi_{\text{sample}}(\cdot) + A_i \sum_{k=0}^T \nabla_{\theta} \log \pi_d(\cdot)]$ The advantage multiplies both gradient sums identically. There is no action-specific immediate reward that could create magnitude asymmetry—both policy components receive gradient signal proportional to their log-probability scores weighted by the *same* scalar A_i . This is the formal sense in which attribution is "balanced." See Appendix A.2 for complete proof. \square

Interpretation. The sufficient statistic $\Phi = \gamma^{\text{len}(\cdot)} A_i$ encodes: "this trajectory will yield advantage A_i at the end, discounted by the temporal distance." Both π_{sample} and π_d use this *same* information when evaluating their actions. This enables coherent learning in the unified network.

3.3.2 KL Penalty: Unbalanced Gradient Attribution

In RLHF and GRPO, the KL divergence penalty regularizes the learned policy π_{θ} against a reference policy π_{ref} (typically the SFT model). Following standard practice, we consider the token-level KL penalty added to the reward:⁹

$$J(\theta) = \mathbb{E}_{\tau \sim \pi_{\theta}} \left[R(\tau) - w \sum_{t=1}^{|\tau|} \log \frac{\pi_{\theta}(a_t | s_t)}{\pi_{\text{ref}}(a_t | s_t)} \right]$$

where $w \geq 0$ controls the regularization strength.

Under our policy decomposition, the per-trajectory KL penalty decomposes as:

$$D_{\text{KL}}^{\text{token}}(\tau) = \underbrace{\sum_{k=1}^T \sum_{j=1}^{L_k} \log \frac{\pi_{\text{sample},\theta}(\text{token}_{k,j} | \cdot)}{\pi_{\text{sample},\text{ref}}(\text{token}_{k,j} | \cdot)}}_{\text{Sampling KL: } \sum_k L_k \text{ terms}} + \underbrace{\sum_{k=1}^T \log \frac{\pi_{d,\theta}(a_k | s_k)}{\pi_{d,\text{ref}}(a_k | s_k)}}_{\text{Decision KL: } T \text{ terms}}$$

The structural asymmetry is immediate: sampling actions contribute $\sum_{k=1}^T L_k$ terms while decision actions contribute only T terms. Since typical reasoning traces have $L_k \gg 1$ (hundreds of tokens per attempt), the sampling component dominates.

Define the immediate KL penalties for each action type:

$$\begin{aligned} d_k^{\text{sample}} &= \sum_{j=1}^{L_k} \log \frac{\pi_{\text{sample},\theta}(\text{token}_{k,j} | \cdot)}{\pi_{\text{sample},\text{ref}}(\text{token}_{k,j} | \cdot)} \sim O(L_k) \\ d_k^{\text{decision}} &= \log \frac{\pi_{d,\theta}(a_k | s_k)}{\pi_{d,\text{ref}}(a_k | s_k)} \sim O(1) \end{aligned}$$

Theorem 3.2. For the token-level KL penalty, the Q-values satisfy the Bellman recursions:

$$\begin{aligned} Q_{\text{sample}}^{\pi,\text{KL}}(s_{k-1}, a'_k) &= d_k^{\text{sample}} + \gamma \cdot \mathbb{E}_{\pi_{\theta}}[Q_d^{\text{KL}}(s_k, a''_k)] \\ Q_d^{\pi,\text{KL}}(s_k, a''_k) &= d_k^{\text{decision}} + \gamma \cdot \mathbb{E}_{\pi_{\theta}}[Q_{\text{sample}}^{\text{KL}}(s_k, a'_{k+1})] \end{aligned}$$

where the immediate penalties satisfy:

$$d_k^{\text{sample}} = \sum_{j=1}^{L_k} \log \frac{\pi_{\text{sample},\theta}(\text{token}_{k,j} | \cdot)}{\pi_{\text{sample},\text{ref}}(\text{token}_{k,j} | \cdot)} \sim O(L_k)$$

⁹This corresponds to the "KL in reward" placement used in GRPO and PPO-based RLHF implementations.

$$d_k^{decision} = \log \frac{\pi_{d,\theta}(a_k|s_k)}{\pi_{d,ref}(a_k|s_k)} \sim O(1)$$

The scale separation $|d_k^{sample}|/|d_k^{decision}| \approx L_k$ creates systematic gradient magnitude asymmetry.

Proof Sketch. The key observation is that d_k^{sample} is a *sum* over L_k token-level divergences, while $d_k^{decision}$ is a single scalar. If individual token-level KL divergences are comparable in magnitude (order δ), then $|d_k^{sample}| \approx L_k \cdot \delta$ while $|d_k^{decision}| \approx \delta$.

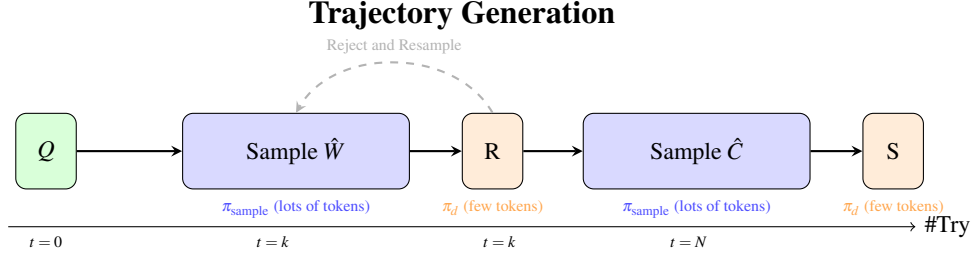
Working backwards from the terminal state: at step T , $Q_d^{KL}(s_T, \text{STOP}) = d_T^{decision} \sim O(1)$. The preceding sampling Q-value is $Q_{sample}^{KL}(s_{T-1}, a'_T) = d_T^{sample} + \gamma \cdot Q_d^{KL}(s_T, \text{STOP}) \approx O(L_T) + O(1) \approx O(L_T)$. The immediate $O(L_k)$ penalty dominates. This asymmetry propagates through the recursion: Q_{sample}^{KL} is dominated by immediate large penalties, while Q_d^{KL} accumulates future sampling penalties but has small immediate terms.

Attempting to define a single sufficient statistic Φ requires satisfying both $\Phi(s_k) \approx O(L_k) + \gamma\Phi(s_{k+1})$ (from sampling) and $\Phi(s_k) \approx O(1) + \gamma\Phi(s_{k+1})$ (from decision). These constraints are inconsistent when $L_k \gg 1$. See Appendix A.5 for the complete proof. \square

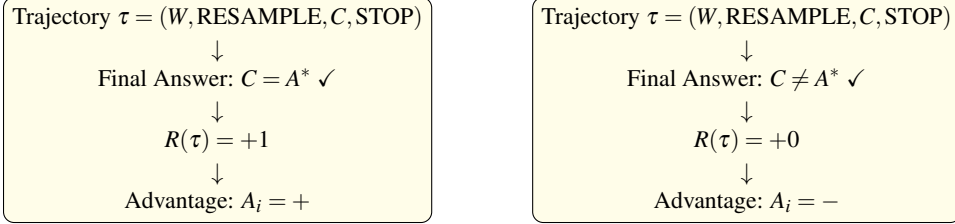
Interpretation. The KL penalty creates asymmetric regularization through its token-level structure. Changes to π_{sample} incur immediate, large penalties proportional to sequence length L_k . Changes to π_d incur small immediate penalties of $O(1)$. When combined with the surrogate reward's symmetric push, the net effect is differential learning: π_d receives sustained positive gradients from the reward with minimal KL constraint, while π_{sample} is heavily regularized toward the reference policy¹⁰.

Remark (Contrast with Surrogate Reward). Under the surrogate reward (Theorem 3.1), both Q-values equal the same length-discounted advantage: $Q_{sample}^{reward} = Q_d^{reward} = \gamma^{\sum \text{len}(\cdot)} A_i$. The advantage multiplies both gradient components equally, creating symmetric learning pressure. The KL penalty lacks this symmetry precisely because the immediate penalties differ by a factor of L_k .

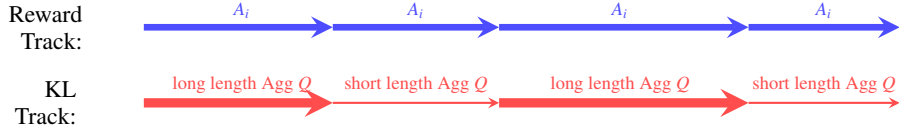
¹⁰We emphasize that the "unbalanced attribution" property does not contradict the existence of a well-defined V^π in the augmented MDP. A unified value function exists by standard theory. Our contribution is characterizing how gradient magnitudes distribute across policy components under different reward structures. The distinction between "balanced" and "unbalanced" is one of degree, specifically, whether immediate reward contributions to different policy components differ by $O(1)$ factors (balanced) or $O(L)$ factors (unbalanced). The latter creates systematic bias in learning dynamics even when a unified value function exists.



Reward Calculation

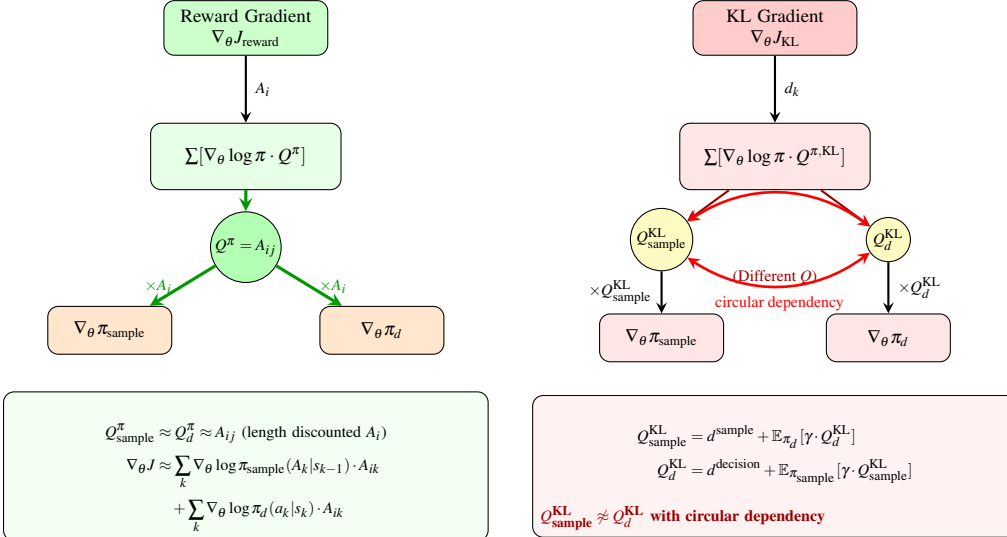


Gradient Propagation



(Surrogate Reward)

(KL Penalty)



Balanced Gradient Attribution

Unbalanced Gradient Attribution

We illustrate the gradient evolution in a simple numerical illustration.¹¹ We parameterize a minimal two-stage process with three learnable logits: θ_s governing sampling accuracy, $\theta_{d|C}$ governing stop decisions given correct answers, and $\theta_{d|W}$ governing resample decisions given incorrect answers.

¹¹The cyclical pattern observed in the training process is because of reference model updating.

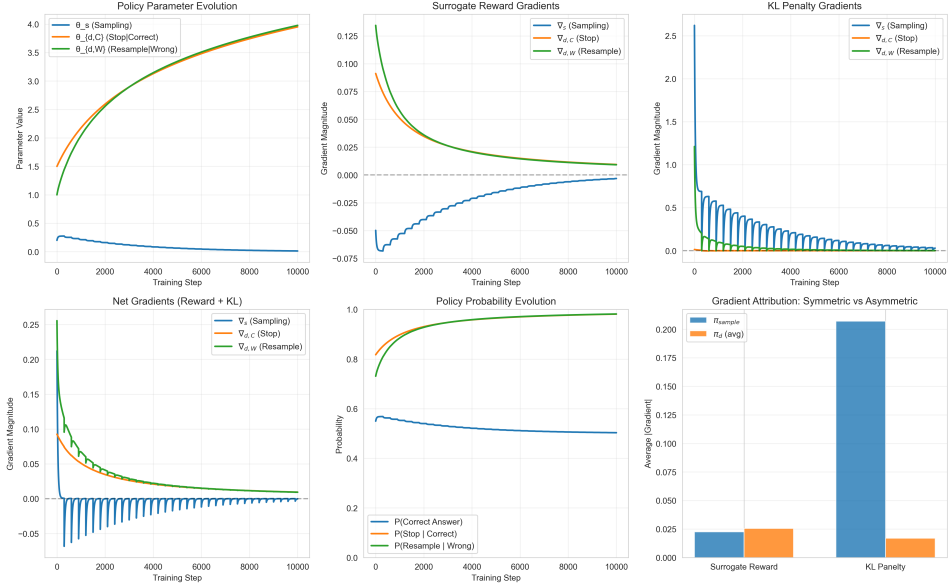


Figure 1: Single Parameter Illustration

Figure 1 displays the training dynamics under the combined GRPO objective. The center panels decompose gradient contributions: the surrogate reward generates comparable gradient magnitudes across all parameters (center-left), while the KL penalty produces gradients for sampling that dominate decision gradients by nearly an order of magnitude (center-right). This confirms the $O(L_k)$ versus $O(1)$ asymmetry established above in the section. The bottom-right panel quantifies this directly—gradient attribution remains symmetric for the surrogate reward but exceeds 2:1 (sampling versus decision) for the KL penalty throughout training.

The net effect (bottom-left) is differential learning: π_d parameters receive sustained positive gradients while π_{sample} is heavily regularized toward the reference. Full derivations appear in Appendix.C.

Remark. Generality of the Gradient Attribution Framework The gradient attribution analysis extends beyond the specific sampling-decision decomposition. Any conceptual partition of a unified policy into sub-policies ($\pi_1, \pi_2, \dots, \pi_K$) that perform functionally distinct operations admits analogous analysis. The core question—whether reward gradients distribute symmetrically or asymmetrically across sub-policies—applies whenever a single optimization objective must simultaneously improve multiple capabilities. Examples include: (i) decomposing into "reasoning" versus "computation" in mathematical problem-solving; (ii) separating "retrieval" from "synthesis" in knowledge-intensive tasks; (iii) distinguishing "planning" from "execution" in multi-step procedures. The gradient attribution property characterizes when such multitasking can be learned coherently versus when length-weighted objectives create systematic imbalances.

4 Experiment and Calibration

The theoretical framework predicts that RL's balanced gradient attribution enables coherent learning of both π_{sample} and π_d , while SFT's imperfect attribution leads to miss-meshed gradients that fail to develop an effective decision policy. We design experiments to validate these predictions and to decompose observed performance gains into their constituent policy components.

4.1 Experimental Setup and Results

Table 1: Model Performance On Arithmetic Tasks

	3×3	3×4	3×5	3×6	3×7	3×8	3×9
Base	74.0 (65.4, 82.6)	34.0 (24.7, 43.3)	5.0 (0.7, 9.3)	1.0 (-1.0, 3.0)	4.0 (0.2, 7.8)	3.0 (-0.3, 6.3)	1.0 (-1.0, 3.0)
SFT (no reflection)	75.0 (66.5, 83.5)	32.0 (22.9, 41.1)	6.0 (1.3, 10.7)	2.0 (-0.7, 4.7)	1.0 (-1.0, 3.0)	0.0 (0.0, 0.0)	1.0 (-1.0, 3.0)
SFT (reflection)	96.0 (92.2, 99.8)	92.0 (86.7, 97.3)	94.0 (89.3, 98.7)	49.0 (39.2, 58.8)	4.0 (0.2, 7.8)	1.0 (-1.0, 3.0)	0.0 (0.0, 0.0)
RL	98.0 (95.3, 100.7)	91.0 (85.4, 96.6)	92.0 (86.7, 97.3)	90.0 (84.1, 95.9)	72.0 (63.2, 80.8)	53.0 (43.2, 62.8)	34.0 (24.7, 43.3)

Note: All models based on Qwen2.5-7B-Instruct (Qwen et al., 2025). SFT (no reflection) trained on Q-A pairs with COT but no retry patterns. SFT (reflection) trained on trajectories with multiple attempts and explicit reflection. We report accuracy and 95% CI ($n = 100$).

Table 1 presents model performance across multiplication tasks of increasing difficulty. The 3×3 and 3×4 tasks constitute the training distribution; all others are out-of-distribution (OOD). Both RL and SFT (reflection) achieve near-ceiling in-distribution performance (96–98% on 3×3 , 91–92% on 3×4) and remain comparable on 3×5 . The critical divergence emerges at 3×6 : RL maintains 90% accuracy while SFT (reflection) drops to 49%. This gap widens dramatically further OOD—on 3×9 , RL achieves 34% versus SFT (reflection)’s 0%.

SFT (reflection) substantially outperforms both Base and SFT (no reflection) across all task difficulties, indicating that reflection-rich training data does improve performance. However, the steep degradation pattern—from 94% on 3×5 to near-zero on 3×7 and beyond—suggests this improvement reflects memorization of in-distribution patterns rather than learned generalization. Later in the section, we develop a statistical approach to estimate the performance of π_{sample} and π_d , decomposing the performance gap between RL and SFT (reflection) into contributions from each policy component.

4.2 A Simple Calibration of the Model

To decompose the performance gap between RL and SFT into contributions from π_{sample} and π_d , we construct a calibration model that abstracts the LLM’s behavior into the two-stage decision-sampling process.

Sampling Accuracy (π_{sample}). We model the sampling policy by a single probability $p_s = P(A_k = A_Q^*)$, representing the likelihood that any given sample is correct.

Decision Policy (π_d). We model the decision policy as a classifier with two parameters:

$$p_{d|C} = P(\text{STOP} \mid A_k = A_Q^*),$$

$$p_{d|W} = P(\text{RESAMPLE} \mid A_k \neq A_Q^*).$$

The parameter $p_{d|C}$ captures the probability of correctly accepting a correct answer; $p_{d|W}$ captures the probability of correctly rejecting an incorrect answer. An effective decision policy requires both to be high. The framework predicts that RL develops high $p_{d|W}$ through the surrogate reward’s Balanced Gradient Attribution¹².

Model Accuracy. Under the two-stage model, overall accuracy is:

$$\text{Model Acc} = \frac{p_s \cdot p_{d|C}}{1 - (p_s \cdot (1 - p_{d|C}) + (1 - p_s) \cdot p_{d|W})}.$$

¹²Also it’s reasonable to conjecture that negative sampling and negative reward would tend to develops high $p_{d|C}$.

We estimate $(p_s, p_{d|C}, p_{d|W})$ from model outputs: p_s from first-attempt accuracy, and the decision parameters from observed stopping and resampling behavior conditional on answer correctness.

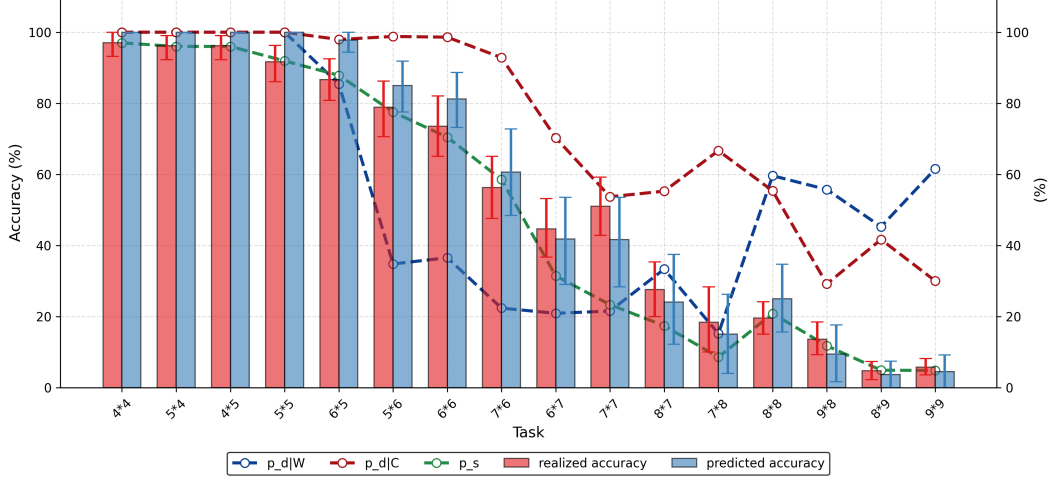


Figure 2: **(RL Thinking Model)**: Calibrated policy parameters across arithmetic task sizes. p_s : sampling accuracy approximated by accuracy of 1st try, $p_{d|C}$: probability of stopping conditional on getting correct answer, $p_{d|W}$: probability of resample conditional on getting incorrect answer.

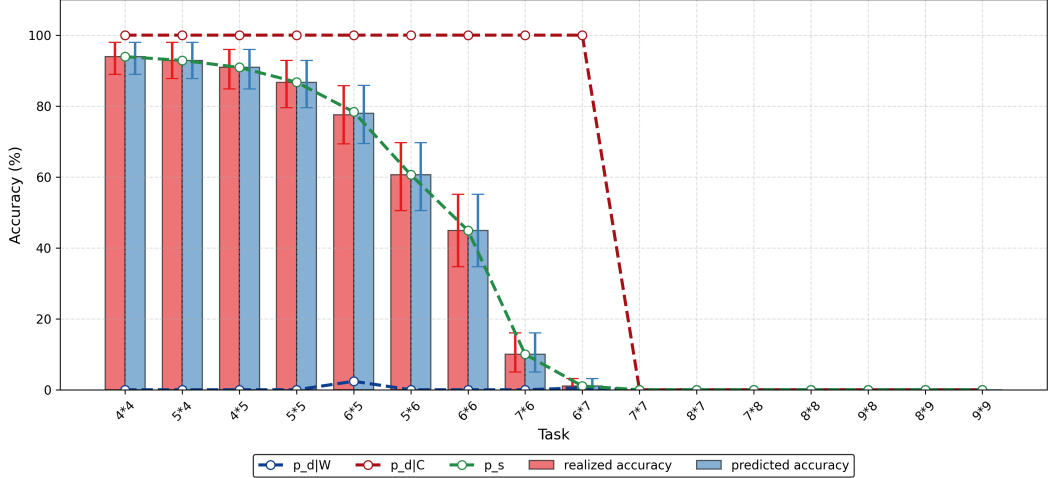


Figure 3: **(SFT Thinking Model)**: Calibrated policy parameters across arithmetic task sizes. p_s : sampling accuracy approximated by accuracy of 1st try, $p_{d|C}$: probability of stopping conditional on getting correct answer, $p_{d|W}$: probability of resample conditional on getting incorrect answer.

Figure 2 presents the calibrated parameters across problem sizes for the RL-trained model. The close agreement between predicted and observed accuracy validates the two-stage decomposition: model behavior is well-characterized by the interaction of sampling quality and decision quality. Three patterns emerge. First, sampling accuracy p_s degrades monotonically with task difficulty, declining from approximately 80% on in-distribution tasks to below 20% on the most challenging OOD tasks. Second, the decision parameters exhibit remarkable stability: $p_{d|C}$ remains near ceiling across all difficulty levels, while $p_{d|W}$ —the probability of correctly rejecting an incorrect answer—sustains values between 40–60% even far out-of-distribution. Third, the calibrated model accurately predicts observed accuracy across the full difficulty range, with predicted and realized values tracking within confidence intervals.

Figure 3 presents the corresponding analysis for the SFT (reflection) model, revealing a starkly different pattern. While $p_{d|C}$ similarly remains high, $p_{d|W}$ collapses toward zero on OOD tasks—the

model fails to reject incorrect answers and instead echoes its first attempts. Sampling accuracy p_s degrades comparably to the RL model on in-distribution tasks but falls more precipitously OOD. The critical distinction lies in the decision policy: RL maintains discriminative ability ($p_{d|W} > 0$) where SFT does not. This confirms the framework’s central prediction—RL’s superior generalization stems primarily from learning an effective π_d , enabling error detection and correction even when π_{sample} falters on harder problems.

5 Towards Understanding the Insufficiency of SFT, and the Power of RL

5.1 SFT Echo Chamber

Recent systematic analysis reveals a striking pattern: SFT consistently fails to develop self-correction capabilities despite extensive efforts to engineer reflection-rich training data. [Kang et al. \(2025\)](#) constructed SFT datasets with varying amounts of reflection steps (cut-at-1 through cut-at-6) and varying proportions of corrective $F \rightarrow T$ transitions (0% to 100%). The results are unambiguous. Models trained on maximum-reflection data outperformed minimal-reflection variants by 4.05%, yet decomposition reveals first-candidate accuracy accounts for 3.75% while reflection contributes only 0.3%. More critically, $p(F \rightarrow T)$ —the probability of correcting an incorrect answer—showed no meaningful improvement across any training configuration. This echoing of first answers, where subsequent reasoning merely confirms rather than corrects, appears universal across SFT-trained thinking models.

Table 2: [Kang et al. \(2025\)](#): FT Training Cannot Improve Self-Correction

F → T Ratio in Data	p(F → T) Llama3.1-8B	p(F → T) Qwen2.5-7B
100%	0.053	0.036
50%	0.058	0.045
0%	0.050	0.041

Note: $p(F \rightarrow T)$ remains flat regardless of corrective reflection exposure.

The gradient attribution framework developed in Section 3 provides a principled explanation. Recall that the surrogate reward exhibits Balanced Gradient Attribution: the advantage A_i acts as a symmetric multiplier attributing credit to whichever policy component was responsible for the outcome. In contrast, SFT operates similarly to a KL-divergence between π_θ and the data distribution π_{data} , exhibiting Unbalanced Gradient Attribution.

The issue is that SFT maximizes likelihood of the entire trajectory as a unified sequence unable to decompose credit between "this was a good decision to RESAMPLE" versus "this was good sampling." Even when training data contains abundant $F \rightarrow T$ corrective patterns, SFT teaches π_{sample} to produce text that resembles reflection but provides no gradient signal for π_d to learn when to trigger correction.

RL’s advantage A_i provides exactly this contrastive signal. Trajectories where the model correctly identifies errors and chooses *RESAMPLE* receive higher reward than those where it incorrectly *STOPs*, creating gradient pressure specifically on the decision component. Explaining the echoing effect that [Kang et al. \(2025\)](#) observes.

5.2 Memorization vs. Generalization.

If SFT primarily improves π_{sample} without developing π_d , it is natural to predict SFT models will memorize training distributions rather than learn generalizable decision rules. [Chu et al. \(2025\)](#) test this directly across four task variants. The results are stark: SFT degrades OOD performance by 8–80% while RL improves it by 3–61%. Crucially, this pattern persists even when SFT uses sub-optimal trajectories containing errors—memorization stems from the training objective’s structure, not data quality.

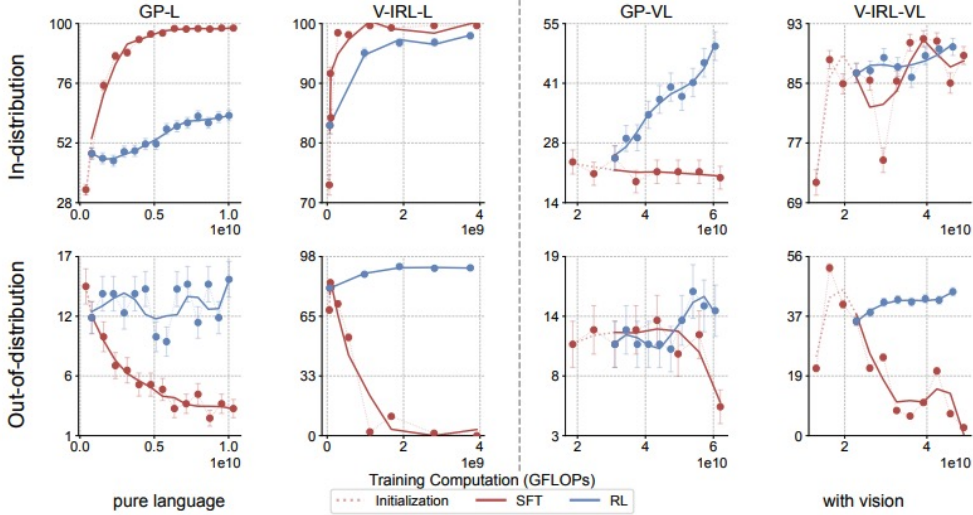


Figure 4: Chu et al. (2025): ID/OOD performance comparison between SFT/RL

5.3 Why do Dynamic Fine-tuning Works Better

Wu et al. (2025) prove that SFT’s gradient is equivalent to policy gradient with an implicit reward inversely proportional to model confidence ($\frac{1}{\pi_\theta}$). Our framework reveals why this is problematic: the $\frac{1}{\pi_\theta}$ weighting creates dense, policy-entangled rewards where the Q-value at each token depends on future policy probabilities, not just future outcomes yielding the impossibility of having a joint Q-function for π_{sample} and π_d ¹³. DFT rescales the objective by π_θ , mitigating the entanglement¹⁴. The effective reward becomes more policy-independent, and Q-values now depend more on trajectory outcomes moving closer to better gradient attribution property. The empirical gains they found are substantial: on Qwen2.5-Math-7B, standard SFT degrades AIME24 from 6.68 to 2.48, while DFT improves it to 8.56, a significant improvement follows directly from simply correcting the Q-function structure.

5.4 The Power of Negative Feedback.

If the key to developing π_d is gradient signal for the RESAMPLE action, methods emphasizing negative samples should prove effective. Zhu et al. (2025) show that Negative Sample Reinforcement (NSR) alone—without any training on correct responses—achieves Pass256 of 96.9% on MATH, comparable to full REINFORCE. Learning from mistakes, which provides precisely the "incorrect state → need to resample" signal absent in SFT, proves surprisingly powerful.

6 Conclusion

We develop the Two-Stage Decision-Sampling Hypothesis as a mechanistic framework for understanding self-reflection in RL-trained LLMs. The core contribution is the gradient attribution property, which characterizes how reward gradients distribute between content generation (π_{sample}) and output verification (π_d). We prove that surrogate rewards exhibit Balanced Gradient Attribution. In contrast, 'KL-like' rewards exhibit Unbalanced Gradient Attribution, inducing miss attribution of gradient among policies mitigating the effectiveness of learning.

Empirical validation on arithmetic reasoning confirms the framework’s predictions. The calibrated two-stage model accurately predicts observed accuracy, and the decomposition reveals that RL’s gains are attributable to improved decision quality (π_d) and improved sampling quality (π_{sample}).

¹³Refer to appendix.A and appendix.B for proof of the Unbalanced Gradient Attribution property of RL penalty.

¹⁴although not fully canceling it because of the length asymmetry, we formally show this in appendix.D.

Specifically, while both RL and SFT models exhibit comparable degradation in sampling accuracy p_s on out-of-distribution tasks, RL maintains substantial $p_{d|W}$ (40–60%) where SFT collapses to near zero—confirming that RL’s superior generalization derives primarily from learning when to reject and retry rather than from improved first-attempt generation. The framework also explains documented phenomena including SFT’s echoing effect, the memorization-versus-generalization distinction, DFT’s effectiveness, and the power of negative samples.

Several limitations merit acknowledgment. The theoretical analysis abstracts away practical considerations such as clipping and trust regions. Empirical validation is conducted on arithmetic reasoning; extension to more complex domains remains future work. The calibration model assumes a simplified two-stage structure that does not fully capture full realistic model behavior such as accuracy deterioration over length generalization.

The gradient attribution framework suggests that training objectives should be designed with attention to their attribution properties. More broadly, the distinction between “learning to generate” and “learning to verify” may be fundamental to understanding thinking models. We hope this framework proves useful for both analyzing existing models and designing training procedures that more effectively develop genuine self-correction capabilities.

Acknowledgments

This work is supported by Shanghai Artificial Intelligence Laboratory and ShanghaiTech University. All error remains our own.

References

Agarwal, A., Kakade, S. M., Lee, J. D., and Mahajan, G. (2020). On the theory of policy gradient methods: Optimality, approximation, and distribution shift.

Anil, C., Wu, Y., Andreassen, A., Lewkowycz, A., Misra, V., Ramasesh, V., Slone, A., Gur-Ari, G., Dyer, E., and Neyshabur, B. (2022). Exploring length generalization in large language models. *Advances in Neural Information Processing Systems*, 35:38546–38556.

Bercovich, A., Levy, I., Golan, I., Dabbah, M., El-Yaniv, R., Puny, O., Galil, I., Moshe, Z., Ronen, T., Nabwani, N., Shahaf, I., Tropp, O., Karpas, E., Zilberstein, R., Zeng, J., Singhal, S., Bukharin, A., Zhang, Y., Konuk, T., Shen, G., Mahabaleshwarkar, A. S., Kartal, B., Suhara, Y., Delalleau, O., Chen, Z., Wang, Z., Mosallanezhad, D., Renduchintala, A., Qian, H., Rekesh, D., Jia, F., Majumdar, S., Noroozi, V., Ahmad, W. U., Narenthiran, S., Ficek, A., Samadi, M., Huang, J., Jain, S., Gitman, I., Moshkov, I., Du, W., Toshniwal, S., Armstrong, G., Kisacanin, B., Novikov, M., Gitman, D., Bakhturina, E., Varshney, P., Narsimhan, M., Scowcroft, J. P., Kamalu, J., Su, D., Kong, K., Kliegl, M., Mahabadi, R. K., Lin, Y., Satheesh, S., Parmar, J., Gundecha, P., Norick, B., Jennings, J., Prabhumoye, S., Akter, S. N., Patwary, M., Khattar, A., Narayanan, D., Waleffe, R., Zhang, J., Su, B.-Y., Huang, G., Kong, T., Chadha, P., Jain, S., Harvey, C., Segal, E., Huang, J., Kashirsky, S., McQueen, R., Putterman, I., Lam, G., Venkatesan, A., Wu, S., Nguyen, V., Kilaru, M., Wang, A., Warne, A., Somasamudramath, A., Bhaskar, S., Dong, M., Assaf, N., Mor, S., Argov, O. U., Junkin, S., Romanenko, O., Larroy, P., Katariya, M., Rovinelli, M., Balas, V., Edelman, N., Bhiwandiwalla, A., Subramaniam, M., Ithape, S., Ramamoorthy, K., Wu, Y., Velury, S. V., Almog, O., Daw, J., Fridman, D., Galinkin, E., Evans, M., Ghosh, S., Luna, K., Derczynski, L., Pope, N., Long, E., Schneider, S., Siman, G., Grzegorzek, T., Ribalta, P., Katariya, M., Alexiuk, C., Conway, J., Saar, T., Guan, A., Pawelec, K., Prayaga, S., Kuchaiev, O., Ginsburg, B., Olabiyi, O., Briski, K., Cohen, J., Catanzaro, B., Alben, J., Geifman, Y., and Chung, E. (2025). Llama-nemotron: Efficient reasoning models.

Chu, T., Zhai, Y., Yang, J., Tong, S., Xie, S., Schuurmans, D., Le, Q. V., Levine, S., and Ma, Y. (2025). Sft memorizes, rl generalizes: A comparative study of foundation model post-training.

Cobbe, K., Kosaraju, V., Bavarian, M., Chen, M., Jun, H., Kaiser, L., Plappert, M., Tworek, J., Hilton, J., Nakano, R., Hesse, C., and Schulman, J. (2021). Training verifiers to solve math word problems.

DeepSeek-AI, Guo, D., et al. (2025). DeepSeek-R1: Incentivizing reasoning capability in LLMs via reinforcement learning. *arXiv preprint arXiv:2501.12948*.

Feng, G., Zhang, B., Gu, Y., Ye, H., He, D., and Wang, L. (2023). Towards revealing the mystery behind chain of thought: A theoretical perspective.

Hendrycks, D., Burns, C., Kadavath, S., Arora, A., Basart, S., Tang, E., Song, D., and Steinhardt, J. (2021). Measuring mathematical problem solving with the math dataset.

Huang, J., Gu, X., Shen, L., Kordi, Y., Wu, B., Zhang, K., Li, D., Li, Q., Zhang, P., Liu, Y., et al. (2024). Large language models cannot self-correct reasoning yet. In *International Conference on Learning Representations*.

Jiang, Y., Xiong, Y., Yuan, Y., Xin, C., Xu, W., Yue, Y., Zhao, Q., and Yan, L. (2025). Pag: Multi-turn reinforced llm self-correction with policy as generative verifier.

Kamoi, R., Golovneva, O., Hsu, P.-Y., Celikyilmaz, A., Kim, Y., Choi, Y., and Freitag, M. (2024). A critical analysis of self-correction capabilities in large language models. *Transactions of the Association for Computational Linguistics*, 12.

Kang, L., Deng, Y., Xiao, Y., Mo, Z., Lee, W. S., and Bing, L. (2025). First try matters: Revisiting the role of reflection in reasoning models.

Kumar, A., Zhuang, V., Agarwal, R., Su, Y., Kazemi, S. M., and Levine, S. (2024). Training language models to self-correct via reinforcement learning. *arXiv preprint arXiv:2409.12917*.

Lee, N., Sreenivasan, K., Lee, J. D., Lee, K., and Papailiopoulos, D. (2023). Teaching arithmetic to small transformers. *arXiv preprint arXiv:2307.03381*.

Ma, R., Wang, P., Liu, C., Liu, X., Chen, J., Zhang, B., Zhou, X., Du, N., and Li, J. (2025). S²r: Teaching llms to self-verify and self-correct via reinforcement learning.

Nogueira, R., Jiang, Z., and Lin, J. (2021). Investigating the limitations of transformers with simple arithmetic tasks. *arXiv preprint arXiv:2102.13019*.

OpenAI, :, Jaech, A., Kalai, A., Lerer, A., Richardson, A., El-Kishky, A., Low, A., Helyar, A., Madry, A., Beutel, A., Carney, A., Iftimie, A., Karpenko, A., Passos, A. T., Neitz, A., Prokofiev, A., Wei, A., Tam, A., Bennett, A., Kumar, A., Saraiva, A., Vallone, A., Duberstein, A., Kondrich, A., Mishchenko, A., Applebaum, A., Jiang, A., Nair, A., Zoph, B., Ghorbani, B., Rossen, B., Sokolowsky, B., Barak, B., McGrew, B., Minaiev, B., Hao, B., Baker, B., Houghton, B., McKinzie, B., Eastman, B., Lugaressi, C., Bassin, C., Hudson, C., Li, C. M., de Bourcy, C., Voss, C., Shen, C., Zhang, C., Koch, C., Orsinger, C., Hesse, C., Fischer, C., Chan, C., Roberts, D., Kappler, D., Levy, D., Selsam, D., Dohan, D., Farhi, D., Mely, D., Robinson, D., Tsipras, D., Li, D., Oprica, D., Freeman, E., Zhang, E., Wong, E., Proehl, E., Cheung, E., Mitchell, E., Wallace, E., Ritter, E., Mays, E., Wang, F., Such, F. P., Raso, F., Leoni, F., Tsimpourlas, F., Song, F., von Lohmann, F., Sulit, F., Salmon, G., Parascandolo, G., Chabot, G., Zhao, G., Brockman, G., Leclerc, G., Salman, H., Bao, H., Sheng, H., Andrin, H., Bagherinezhad, H., Ren, H., Lightman, H., Chung, H. W., Kivlichan, I., O'Connell, I., Osband, I., Gilaberte, I. C., Akkaya, I., Kostrikov, I., Sutskever, I., Kofman, I., Pachocki, J., Lennon, J., Wei, J., Harb, J., Twore, J., Feng, J., Yu, J., Weng, J., Tang, J., Yu, J., Candela, J. Q., Palermo, J., Parish, J., Heidecke, J., Hallman, J., Rizzo, J., Gordon, J., Uesato, J., Ward, J., Huizinga, J., Wang, J., Chen, K., Xiao, K., Singhal, K., Nguyen, K., Cobbe, K., Shi, K., Wood, K., Rimbach, K., Gu-Lemberg, K., Liu, K., Lu, K., Stone, K., Yu, K., Ahmad, L., Yang, L., Liu, L., Maksin, L., Ho, L., Fedus, L., Weng, L., Li, L., McCallum, L., Held, L., Kuhn, L., Kondraciuk, L., Kaiser, L., Metz, L., Boyd, M., Trebacz, M., Joglekar, M., Chen, M., Tintor, M., Meyer, M., Jones, M., Kaufer, M., Schwarzer, M., Shah, M., Yatbaz, M., Guan, M. Y., Xu, M., Yan, M., Glaese, M., Chen, M., Lampe, M., Malek, M., Wang, M., Fradin, M., McClay, M., Pavlov, M., Wang, M., Wang, M., Murati, M., Bavarian, M., Rohaninejad, M., McAleese, N., Chowdhury, N., Chowdhury, N., Ryder, N., Tezak, N., Brown, N., Nachum, O., Boiko, O., Murk, O., Watkins, O., Chao, P., Ashbourne, P., Izmailov, P., Zhokhov, P., Dias, R., Arora, R., Lin, R., Lopes, R. G., Gaon, R., Miyara, R., Leike, R., Hwang, R., Garg, R., Brown, R., James, R., Shu, R., Cheu, R., Greene, R., Jain, S., Altman, S., Toizer, S., Toyer, S., Miserendino, S., Agarwal, S., Hernandez, S., Baker, S., McKinney, S., Yan, S., Zhao, S., Hu, S., Santurkar, S., Chaudhuri, S. R., Zhang, S., Fu, S., Papay, S., Lin, S., Balaji, S., Sanjeev, S., Sidor, S., Broda, T., Clark, A., Wang, T., Gordon, T., Sanders, T., Patwardhan, T., Sottiaux, T., Degry, T., Dimson, T., Zheng, T., Garipov, T., Stasi, T., Bansal, T., Creech, T., Peterson, T., Eloundou, T., Qi, V., Kosaraju, V., Monaco, V., Pong,

V., Fomenko, V., Zheng, W., Zhou, W., McCabe, W., Zaremba, W., Dubois, Y., Lu, Y., Chen, Y., Cha, Y., Bai, Y., He, Y., Zhang, Y., Wang, Y., Shao, Z., and Li, Z. (2024). Openai o1 system card.

Ouyang, L., Wu, J., Jiang, X., Almeida, D., Wainwright, C. L., Mishkin, P., Zhang, C., Agarwal, S., Slama, K., Ray, A., Schulman, J., Hilton, J., Kelton, F., Miller, L., Simens, M., Askell, A., Welinder, P., Christiano, P., Leike, J., and Lowe, R. (2022). Training language models to follow instructions with human feedback.

Phan, L., Gatti, A., Han, Z., Li, N., Hu, J., Zhang, H., Zhang, C. B. C., Shaaban, M., Ling, J., Shi, S., Choi, M., Agrawal, A., Chopra, A., Khoja, A., Kim, R., Ren, R., Hausenloy, J., Zhang, O., Mazeika, M., Dodonov, D., Nguyen, T., Lee, J., Anderson, D., Doroshenko, M., Stokes, A. C., Mahmood, M., Pokutnyi, O., Iskra, O., Wang, J. P., Levin, J.-C., Kazakov, M., Feng, F., Feng, S. Y., Zhao, H., Yu, M., Gangal, V., Zou, C., Wang, Z., Popov, S., Gerbicz, R., Galgon, G., Schmitt, J., Yeadon, W., Lee, Y., Sauers, S., Sanchez, A., Giska, F., Roth, M., Riis, S., Utpala, S., Burns, N., Goshu, G. M., Naiya, M. M., Agu, C., Giboney, Z., Cheatom, A., Fournier-Facio, F., Crowson, S.-J., Finke, L., Cheng, Z., Zampese, J., Hoerr, R. G., Nandor, M., Park, H., Gehrunger, T., Cai, J., McCarty, B., Garretson, A. C., Taylor, E., Sileo, D., Ren, Q., Qazi, U., Li, L., Nam, J., Wydallis, J. B., Arkhipov, P., Shi, J. W. L., Bacho, A., Willcocks, C. G., Cao, H., Motwani, S., de Oliveira Santos, E., Veith, J., Vendrow, E., Cojoc, D., Zenitani, K., Robinson, J., Tang, L., Li, Y., Vendrow, J., Fraga, N. W., Kuchkin, V., Maksimov, A. P., Marion, P., Efremov, D., Lynch, J., Liang, K., Mikov, A., Gritsevskiy, A., Guillod, J., Demir, G., Martinez, D., Pageler, B., Zhou, K., Soori, S., Press, O., Tang, H., Rissone, P., Green, S. R., Brüssel, L., Twayana, M., Dieuleveut, A., Imperial, J. M., Prabhu, A., Yang, J., Crispino, N., Rao, A., Zvonkine, D., Loiseau, G., Kalinin, M., Lukas, M., Manolescu, C., Stambaugh, N., Mishra, S., Hogg, T., Bosio, C., Coppola, B. P., Salazar, J., Jin, J., Sayous, R., Ivanov, S., Schwaller, P., Senthilkuma, S., Bran, A. M., Algaba, A., den Houte, K. V., Sypt, L. V. D., Verbeken, B., Noever, D., Kopylov, A., Myklebust, B., Li, B., Schut, L., Zheltonozhskii, E., Yuan, Q., Lim, D., Stanley, R., Yang, T., Maar, J., Wykowski, J., Oller, M., Sahu, A., Ardito, C. G., Hu, Y., Kamdoum, A. G. K., Jin, A., Vilchis, T. G., Zu, Y., Lackner, M., Koppel, J., Sun, G., Antonenko, D. S., Chern, S., Zhao, B., Arsene, P., Cavanagh, J. M., Li, D., Shen, J., Crisostomi, D., Zhang, W., Dehghan, A., Ivanov, S., Perrella, D., Kaparov, N., Zang, A., Sucholutsky, I., Kharlamova, A., Orel, D., Poritski, V., Ben-David, S., Berger, Z., Whitfill, P., Foster, M., Munro, D., Ho, L., Sivarajan, S., Hava, D. B., Kuchkin, A., Holmes, D., Rodriguez-Romero, A., Sommerhage, F., Zhang, A., Moat, R., Schneider, K., Kazibwe, Z., Clarke, D., Kim, D. H., Dias, F. M., Fish, S., Elser, V., Kreiman, T., Vilchis, V. E. G., Klose, I., Anantheswaran, U., Zweiger, A., Rawal, K., Li, J., Nguyen, J., Daans, N., Heidinger, H., Radionov, M., Rozhoň, V., Ginis, V., Stump, C., Cohen, N., Poświaty, R., Tkadlec, J., Goldfarb, A., Wang, C., Padlewski, P., Barzowski, S., Montgomery, K., Stendall, R., Tucker-Foltz, J., Stade, J., Rogers, T. R., Goertzen, T., Grabb, D., Shukla, A., Givré, A., Ambay, J. A., Sen, A., Aziz, M. F., Inlow, M. H., He, H., Zhang, L., Kaddar, Y., Ängquist, I., Chen, Y., Wang, H. K., Ramakrishnan, K., Thornley, E., Terpin, A., Schoelkopf, H., Zheng, E., Carmi, A., Brown, E. D. L., Zhu, K., Bartolo, M., Wheeler, R., Stehberger, M., Bradshaw, P., Heimonen, J., Sridhar, K., Akov, I., Sandlin, J., Makarychev, Y., Tam, J., Hoang, H., Cunningham, D. M., Goryachev, V., Patramanis, D., Krause, M., Redenti, A., Aldous, D., Lai, J., Coleman, S., Xu, J., Lee, S., Magoulas, I., Zhao, S., Tang, N., Cohen, M. K., Paradise, O., Kirchner, J. H., Ovchinnikov, M., Matos, J. O., Shenoy, A., Wang, M., Nie, Y., Sztyber-Betley, A., Faraboschi, P., Riblet, R., Crozier, J., Halasyamani, S., Verma, S., Joshi, P., Meril, E., Ma, Z., Andréoletti, J., Singhal, R., Platnick, J., Nevirkovets, V., Basler, L., Ivanov, A., Khouri, S., Gustafsson, N., Piccardo, M., Mostaghimi, H., Chen, Q., Singh, V., Khánh, T. Q., Rosu, P., Szlyk, H., Brown, Z., Narayan, H., Menezes, A., Roberts, J., Alley, W., Sun, K., Patel, A., Lamparth, M., Reuel, A., Xin, L., Xu, H., Loader, J., Martin, F., Wang, Z., Achilleos, A., Preu, T., Korbak, T., Bosio, I., Kazemi, F., Chen, Z., Bálint, B., Lo, E. J. Y., Wang, J., Nunes, M. I. S., Milbauer, J., Bari, M. S., Wang, Z., Ansarinejad, B., Sun, Y., Durand, S., Elgnainy, H., Douville, G., Tordera, D., Balabanian, G., Wolff, H., Kvistad, L., Milliron, H., Sakor, A., Eron, M., O., A. F. D., Shah, S., Zhou, X., Kamalov, F., Abdoli, S., Santens, T., Barkan, S., Tee, A., Zhang, R., Tomasiello, A., Luca, G. B. D., Looi, S.-Z., Le, V.-K., Kolt, N., Pan, J., Rodman, E., Drori, J., Fossum, C. J., Muennighoff, N., Jagota, M., Pradeep, R., Fan, H., Eicher, J., Chen, M., Thaman, K., Merrill, W., Firsching, M., Harris, C., Ciobâcă, S., Gross, J., Pandey, R., Gusev, I., Jones, A., Agnihotri, S., Zhelnov, P., Mofayzei, M., Piperski, A., Zhang, D. K., Dobarskyi, K., Leventov, R., Soroko, I., Duersch, J., Taamazyan, V., Ho, A., Ma, W., Held, W., Xian, R., Zebaze, A. R., Mohamed, M., Leser, J. N., Yuan, M. X., Yacar, L., Lengler, J., Olszewska, K., Fratta, C. D., Oliveira, E., Jackson, J. W., Zou, A., Chidambaram, M., Manik, T., Haffenden, H., Stander, D.,

Dasouqi, A., Shen, A., Golshani, B., Stap, D., Kretov, E., Uzhou, M., Zhidkovskaya, A. B., Winter, N., Rodriguez, M. O., Lauff, R., Wehr, D., Tang, C., Hossain, Z., Phillips, S., Samuele, F., Ekström, F., Hammon, A., Patel, O., Farhidi, F., Medley, G., Mohammadzadeh, F., Peñaflor, M., Kassahun, H., Friedrich, A., Perez, R. H., Pyda, D., Sakal, T., Dhamane, O., Mirabadi, A. K., Hallman, E., Okutsu, K., Battaglia, M., Maghsoudimehrabani, M., Amit, A., Hulbert, D., Pereira, R., Weber, S., Handoko, Peristyy, A., Malina, S., Mehkary, M., Aly, R., Reidegeld, F., Dick, A.-K., Friday, C., Singh, M., Shapourian, H., Kim, W., Costa, M., Gurdogan, H., Kumar, H., Ceconello, C., Zhuang, C., Park, H., Carroll, M., Tawfeek, A. R., Steinerberger, S., Aggarwal, D., Kirchhof, M., Dai, L., Kim, E., Ferret, J., Shah, J., Wang, Y., Yan, M., Burdzy, K., Zhang, L., Franca, A., Pham, D. T., Loh, K. Y., Robinson, J., Jackson, A., Giordano, P., Petersen, P., Cosma, A., Colino, J., White, C., Votava, J., Vinnikov, V., Delaney, E., Spelda, P., Stritecky, V., Shahid, S. M., Mourrat, J.-C., Vetoshkin, L., Sponselee, K., Bacho, R., Yong, Z.-X., de la Rosa, F., Cho, N., Li, X., Malod, G., Weller, O., Albani, G., Lang, L., Laurendeau, J., Kazakov, D., Adesanya, F., Portier, J., Hollom, L., Souza, V., Zhou, Y. A., Degorre, J., Yalın, Y., Obikoya, G. D., Rai, Bigi, F., Boscá, M. C., Shumar, O., Bacho, K., Recchia, G., Popescu, M., Shulga, N., Tanwie, N. M., Lux, T. C. H., Rank, B., Ni, C., Brooks, M., Yakimchyk, A., Huanxu, Liu, Cavalleri, S., Häggström, O., Verkama, E., Newbould, J., Gundlach, H., Brito-Santana, L., Amaro, B., Vajipey, V., Grover, R., Wang, T., Kratish, Y., Li, W.-D., Gopi, S., Caciolai, A., de Witt, C. S., Hernández-Cámarra, P., Rodolà, E., Robins, J., Williamson, D., Cheng, V., Raynor, B., Qi, H., Segev, B., Fan, J., Martinson, S., Wang, E. Y., Hausknecht, K., Brenner, M. P., Mao, M., Demian, C., Kassani, P., Zhang, X., Avagian, D., Scipio, E. J., Ragoler, A., Tan, J., Sims, B., Plecnik, R., Kirtland, A., Bodur, O. F., Shinde, D. P., Labrador, Y. C. L., Adoul, Z., Zekry, M., Karakoc, A., Santos, T. C. B., Shamseldeen, S., Karim, L., Liakhovitskaia, A., Resman, N., Farina, N., Gonzalez, J. C., Maayan, G., Anderson, E., Pena, R. D. O., Kelley, E., Mariji, H., Pouriamanesh, R., Wu, W., Finocchio, R., Alarab, I., Cole, J., Ferreira, D., Johnson, B., Safdari, M., Dai, L., Arthornthurasuk, S., McAlister, I. C., Moyano, A. J., Pronin, A., Fan, J., Ramirez-Trinidad, A., Malysheva, Y., Pottmaier, D., Taheri, O., Stepanic, S., Perry, S., Askew, L., Rodríguez, R. A. H., Minissi, A. M. R., Lorena, R., Iyer, K., Fasiludeen, A. A., Clark, R., Ducey, J., Piza, M., Somrak, M., Vergo, E., Qin, J., Borbás, B., Chu, E., Lindsey, J., Jallon, A., McInnis, I. M. J., Chen, E., Semler, A., Gloor, L., Shah, T., Carauleanu, M., Lauer, P., Đuc Huy, T., Shahrtash, H., Duc, E., Lewark, L., Brown, A., Albanie, S., Weber, B., Vaz, W. S., Clavier, P., Fan, Y., e Silva, G. P. R., Long, Lian, Abramovitch, M., Jiang, X., Mendoza, S., Islam, M., Gonzalez, J., Mavroudis, V., Xu, J., Kumar, P., Goswami, L. P., Bugas, D., Heydari, N., Jeanplong, F., Jansen, T., Pinto, A., Apronti, A., Galal, A., Ze-An, N., Singh, A., Jiang, T., of Arc Xavier, J., Agarwal, K. P., Berkani, M., Zhang, G., Du, Z., de Oliveira Junior, B. A., Malishev, D., Remy, N., Hartman, T. D., Tarver, T., Mensah, S., Loume, G. A., Morak, W., Habibi, F., Hoback, S., Cai, W., Gimenez, J., Montecillo, R. G., Łucki, J., Campbell, R., Sharma, A., Meer, K., Gul, S., Gonzalez, D. E., Alapont, X., Hoover, A., Chhablani, G., Vargus, F., Agarwal, A., Jiang, Y., Patil, D., Outevsky, D., Scaria, K. J., Maheshwari, R., Dendane, A., Shukla, P., Cartwright, A., Bogdanov, S., Mündler, N., Möller, S., Arnaboldi, L., Thaman, K., Siddiqi, M. R., Saxena, P., Gupta, H., Fruhauff, T., Sherman, G., Vincze, M., Usawasutsakorn, S., Ler, D., Radhakrishnan, A., Enyekwe, I., Salauddin, S. M., Muzhen, J., Maksapetyan, A., Rossbach, V., Harjadi, C., Bahaloohoreh, M., Sparrow, C., Sidhu, J., Ali, S., Bian, S., Lai, J., Singer, E., Uro, J. L., Bateman, G., Sayed, M., Menshawy, A., Duclosel, D., Bezzi, D., Jain, Y., Aaron, A., Tiryakioglu, M., Siddh, S., Krenek, K., Shah, I. A., Jin, J., Creighton, S., Peskoff, D., EL-Wasif, Z., V, R. P., Richmond, M., McGowan, J., Patwardhan, T., Sun, H.-Y., Sun, T., Zubić, N., Sala, S., Ebert, S., Kaddour, J., Schottdorf, M., Wang, D., Petruzella, G., Meiburg, A., Medved, T., ElSheikh, A., Hebbar, S. A., Vaquero, L., Yang, X., Poulos, J., Zouhar, V., Bogdanik, S., Zhang, M., Sanz-Ros, J., Anugraha, D., Dai, Y., Nhu, A. N., Wang, X., Demircali, A. A., Jia, Z., Zhou, Y., Wu, J., He, M., Chandok, N., Sinha, A., Luo, G., Le, L., Noyé, M., Perelkiewicz, M., Pantidis, I., Qi, T., Purohit, S. S., Parcalabescu, L., Nguyen, T.-H., Winata, G. I., Ponti, E. M., Li, H., Dhole, K., Park, J., Abbondanza, D., Wang, Y., Nayak, A., Caetano, D. M., Wong, A. A. W. L., del Rio-Chanona, M., Kondor, D., Francois, P., Chalstrey, E., Zsambok, J., Hoyer, D., Reddish, J., Hauser, J., Rodrigo-Ginés, F.-J., Datta, S., Shepherd, M., Kamphuis, T., Zhang, Q., Kim, H., Sun, R., Yao, J., Dernoncourt, F., Krishna, S., Rismanchian, S., Pu, B., Pinto, F., Wang, Y., Shridhar, K., Overholt, K. J., Briia, G., Nguyen, H., David, Bartomeu, S., Pang, T. C., Wecker, A., Xiong, Y., Li, F., Huber, L. S., Jaeger, J., Maddalena, R. D., Lù, X. H., Zhang, Y., Beger, C., Kon, P. T. J., Li, S., Sanker, V., Yin, M., Liang, Y., Zhang, X., Agrawal, A., Yifei, L. S., Zhang, Z., Cai, M., Sonmez, Y., Cozianu, C., Li, C., Slen, A., Yu, S., Park, H. K., Sarti, G., Briański, M., Stolfo, A., Nguyen, T. A., Zhang, M., Perlitz, Y., Hernandez-Orallo, J., Li, R., Shabani, A., Juefei-Xu, F., Dhingra, S., Zohar, O., Nguyen, M. C., Pondaven, A., Yilmaz, A., Zhao,

X., Jin, C., Jiang, M., Todoran, S., Han, X., Kreuer, J., Rabern, B., Plassart, A., Maggetti, M., Yap, L., Geirhos, R., Kean, J., Wang, D., Mollaei, S., Sun, C., Yin, Y., Wang, S., Li, R., Chang, Y., Wei, A., Bizeul, A., Wang, X., Arrais, A. O., Mukherjee, K., Chamorro-Padial, J., Liu, J., Qu, X., Guan, J., Bouyamour, A., Wu, S., Plomecka, M., Chen, J., Tang, M., Deng, J., Subramanian, S., Xi, H., Chen, H., Zhang, W., Ren, Y., Tu, H., Kim, S., Chen, Y., Marjanović, S. V., Ha, J., Luczyna, G., Ma, J. J., Shen, Z., Song, D., Zhang, C. E., Wang, Z., Gendron, G., Xiao, Y., Smucker, L., Weng, E., Lee, K. H., Ye, Z., Ermon, S., Lopez-Miguel, I. D., Knights, T., Gitter, A., Park, N., Wei, B., Chen, H., Pai, K., Elkhany, A., Lin, H., Siedler, P. D., Fang, J., Mishra, R., Zsolnai-Fehér, K., Jiang, X., Khan, S., Yuan, J., Jain, R. K., Lin, X., Peterson, M., Wang, Z., Malusare, A., Tang, M., Gupta, I., Fosin, I., Kang, T., Dworakowska, B., Matsumoto, K., Zheng, G., Sewuster, G., Villanueva, J. P., Rannev, I., Chernyavsky, I., Chen, J., Banik, D., Racz, B., Dong, W., Wang, J., Bashmal, L., Gonçalves, D. V., Hu, W., Bar, K., Bohdal, O., Patlan, A. S., Dhuliawala, S., Geirhos, C., Wist, J., Kansal, Y., Chen, B., Tire, K., Yücel, A. T., Christof, B., Singla, V., Song, Z., Chen, S., Ge, J., Ponkshe, K., Park, I., Shi, T., Ma, M. Q., Mak, J., Lai, S., Moulin, A., Cheng, Z., Zhu, Z., Zhang, Z., Patil, V., Jha, K., Men, Q., Wu, J., Zhang, T., Vieira, B. H., Aji, A. F., Chung, J.-W., Mahfoud, M., Hoang, H. T., Sperzel, M., Hao, W., Meding, K., Xu, S., Kostakos, V., Manini, D., Liu, Y., Toukmaji, C., Paek, J., Yu, E., Demircali, A. E., Sun, Z., Dewerpe, I., Qin, H., Pflugfelder, R., Bailey, J., Morris, J., Heilala, V., Rosset, S., Yu, Z., Chen, P. E., Yeo, W., Jain, E., Yang, R., Chigurupati, S., Chernyavsky, J., Reddy, S. P., Venugopalan, S., Batra, H., Park, C. F., Tran, H., Maximiano, G., Zhang, G., Liang, Y., Shiyu, H., Xu, R., Pan, R., Suresh, S., Liu, Z., Gulati, S., Zhang, S., Turchin, P., Bartlett, C. W., Scotese, C. R., Cao, P. M., Wu, B., Karwowski, J., Scaramuzza, D., Nattanmai, A., McKellips, G., Cheraku, A., Suhail, A., Luo, E., Deng, M., Luo, J., Zhang, A., Jindel, K., Paek, J., Halevy, K., Baranov, A., Liu, M., Avadhanam, A., Zhang, D., Cheng, V., Ma, B., Fu, E., Do, L., Lass, J., Yang, H., Sunkari, S., Bharath, V., Ai, V., Leung, J., Agrawal, R., Zhou, A., Chen, K., Kalpathi, T., Xu, Z., Wang, G., Xiao, T., Maung, E., Lee, S., Yang, R., Yue, R., Zhao, B., Yoon, J., Sun, S., Singh, A., Luo, E., Peng, C., Osbey, T., Wang, T., Echeazu, D., Yang, H., Wu, T., Patel, S., Kulkarni, V., Sundarapandian, V., Zhang, A., Le, A., Nasim, Z., Yalam, S., Kasamsetty, R., Samal, S., Yang, H., Sun, D., Shah, N., Saha, A., Zhang, A., Nguyen, L., Nagumalli, L., Wang, K., Zhou, A., Wu, A., Luo, J., Telluri, A., Yue, S., Wang, A., and Hendrycks, D. (2025). Humanity's last exam.

Qwen, :, Yang, A., Yang, B., Zhang, B., Hui, B., Zheng, B., Yu, B., Li, C., Liu, D., Huang, F., Wei, H., Lin, H., Yang, J., Tu, J., Zhang, J., Yang, J., Yang, J., Zhou, J., Lin, J., Dang, K., Lu, K., Bao, K., Yang, K., Yu, L., Li, M., Xue, M., Zhang, P., Zhu, Q., Men, R., Lin, R., Li, T., Tang, T., Xia, T., Ren, X., Ren, X., Fan, Y., Su, Y., Zhang, Y., Wan, Y., Liu, Y., Cui, Z., Zhang, Z., and Qiu, Z. (2025). Qwen2.5 technical report.

Rafailov, R., Sharma, A., Mitchell, E., Ermon, S., Manning, C. D., and Finn, C. (2024). Direct preference optimization: Your language model is secretly a reward model.

Schulman, J., Levine, S., Moritz, P., Jordan, M. I., and Abbeel, P. (2017a). Trust region policy optimization.

Schulman, J., Wolski, F., Dhariwal, P., Radford, A., and Klimov, O. (2017b). Proximal policy optimization algorithms.

Shao, Z., Wang, P., Zhu, Q., Xu, R., Song, J., Zhang, M., Li, Y., Wu, Y., and Guo, D. (2024). DeepSeekMath: Pushing the limits of mathematical reasoning in open language models. *arXiv preprint arXiv:2402.03300*.

Sheng, G., Zhang, C., Ye, Z., Wu, X., Zhang, W., Zhang, R., Peng, Y., Lin, H., and Wu, C. (2024). Hybridflow: A flexible and efficient rlhf framework. *arXiv preprint arXiv: 2409.19256*.

Stiennon, N., Ouyang, L., Wu, J., Ziegler, D., Lowe, R., Voss, C., Radford, A., Amodei, D., and Christiano, P. F. (2020). Learning to summarize with human feedback. *Advances in Neural Information Processing Systems*, 33:3008–3021.

Sutton, R. S., McAllester, D. A., Singh, S. P., and Mansour, Y. (1999a). Policy gradient methods for reinforcement learning with function approximation. *Advances in Neural Information Processing Systems*, 12.

Sutton, R. S., Precup, D., and Singh, S. (1999b). Between mdps and semi-mdps: A framework for temporal abstraction in reinforcement learning. *Artificial Intelligence*, 112(1):181–211.

Tang, Z., Zhang, X., Wang, B., and Wei, F. (2024). Mathscale: Scaling instruction tuning for mathematical reasoning.

Wei, J., Wang, X., Schuurmans, D., Bosma, M., Ichter, B., Xia, F., Chi, E., Le, Q. V., and Zhou, D. (2022). Chain-of-thought prompting elicits reasoning in large language models. *Advances in Neural Information Processing Systems*, 35:24824–24837.

Wu, Y., Zhou, Y., Ziheng, Z., Peng, Y., Ye, X., Hu, X., Zhu, W., Qi, L., Yang, M.-H., and Yang, X. (2025). On the generalization of sft: A reinforcement learning perspective with reward rectification.

Xiong, W., Zhang, H., Ye, C., Chen, L., Jiang, N., and Zhang, T. (2025). Self-rewarding correction for mathematical reasoning.

Xu, X., Zhao, Z., Zhang, H., and Yang, Y. (2025). Principled understanding of generalization for generative transformer models in arithmetic reasoning tasks. In *Proceedings of the 63rd Annual Meeting of the Association for Computational Linguistics*. To appear.

Yu, L., Jiang, W., Shi, H., Yu, J., Liu, Z., Zhang, Y., Kwok, J. T., Li, Z., Weller, A., and Liu, W. (2024). Metamath: Bootstrap your own mathematical questions for large language models.

Zhao, X., Xu, T., Wang, X., Chen, Z., Jin, D., Tan, L., Yen-Ting, Yu, Z., Zhao, Z., He, Y., Wang, S., Fang, H., Chandar, S., and Zhu, C. (2025). Boosting llm reasoning via spontaneous self-correction.

Zhao, Y., Yin, H., Zeng, B., Wang, H., Shi, T., Lyu, C., Wang, L., Luo, W., and Zhang, K. (2024). Marco-o1: Towards open reasoning models for open-ended solutions.

Zheng, Y., Zhang, R., Zhang, J., Ye, Y., Luo, Z., Feng, Z., and Ma, Y. (2024). Llamafactory: Unified efficient fine-tuning of 100+ language models. In *Proceedings of the 62nd Annual Meeting of the Association for Computational Linguistics (Volume 3: System Demonstrations)*, Bangkok, Thailand. Association for Computational Linguistics.

Zhu, X., Xia, M., Wei, Z., Chen, W.-L., Chen, D., and Meng, Y. (2025). The surprising effectiveness of negative reinforcement in llm reasoning.

A Proofs for Gradient Attribution Property Framework

This appendix provides complete mathematical derivations for all results in Section 3.

A.1 Proof of Lemma 3.1 (Trajectory Factorization)

Proof. We prove this by applying the chain rule of probability to the sequential generation process. A trajectory τ of length T is:

$$\tau = (A_1, T_1, a_1, A_2, T_2, a_2, \dots, A_T, T_T, a_T)$$

where $a_k \in \{\text{RESAMPLE}, \text{STOP}\}$ for $k = 1, \dots, T-1$ and $a_T = \text{STOP}$ (by definition, the trajectory ends with STOP).

By the chain rule:

$$P(\tau|Q; \theta) = P(A_1, T_1|Q; \theta) \cdot P(a_1|A_1, T_1, Q; \theta) \cdot P(A_2, T_2|a_1, A_1, T_1, Q; \theta) \cdots$$

Sequentially we write it to be:

$$\begin{aligned} P(\tau|Q; \theta) &= \pi_{\text{sample}}(A_1, T_1|s_0; \theta) \cdot \pi_d(\text{RESAMPLE}|s_1; \theta) \cdot \pi_{\text{sample}}(A_2, T_2|s_1; \theta) \\ &\quad \cdots \pi_d(\text{RESAMPLE}|s_{T-1}; \theta) \cdot \pi_{\text{sample}}(A_T, T_T|s_{T-1}; \theta) \cdot \pi_d(\text{STOP}|s_T; \theta) \end{aligned}$$

Thus:

$$P(\tau|Q; \theta) = \left[\prod_{k=1}^T \pi_{\text{sample}}(A_k, T_k|s_{k-1}; \theta) \right] \cdot \left[\prod_{k=1}^{T-1} \pi_d(\text{RESAMPLE}|s_k; \theta) \right] \cdot \pi_d(\text{STOP}|s_T; \theta)$$

□

A.2 Proof of Corollary 3.1 (Gradient Decomposition)

Proof. From Lemma 3.1:

$$\log P(\tau|Q; \theta) = \sum_{k=1}^T \log \pi_{\text{sample}}(A_k, T_k|s_{k-1}; \theta) + \sum_{k=1}^{T-1} \log \pi_d(\text{RESAMPLE}|s_k; \theta) + \log \pi_d(\text{STOP}|s_T; \theta)$$

Taking the gradient with respect to θ :

$$\nabla_{\theta} \log P(\tau|Q; \theta) = \sum_{k=1}^T \nabla_{\theta} \log \pi_{\text{sample}}(A_k, T_k|s_{k-1}; \theta) + \sum_{k=1}^{T-1} \nabla_{\theta} \log \pi_d(\text{RESAMPLE}|s_k; \theta) + \nabla_{\theta} \log \pi_d(\text{STOP}|s_T; \theta)$$

Rewrite the decision gradient more compactly by defining:

- $a_k = \text{RESAMPLE}$ for $k = 1, \dots, T-1$
- $a_T = \text{STOP}$
- $a_0 = \text{START}$ (initial action, could be included for notational completeness)

Then:

$$\nabla_{\theta} \log P(\tau|Q; \theta) = \sum_{k=1}^T \nabla_{\theta} \log \pi_{\text{sample}}(A_k, T_k|s_{k-1}; \theta) + \sum_{k=0}^T \nabla_{\theta} \log \pi_d(a_k|s_k; \theta)$$

where we interpret $\pi_d(a_0|s_0) = 1$ (deterministic start) and thus $\nabla_{\theta} \log \pi_d(a_0|s_0) = 0$. This completes the proof. □

A.3 Proof of Lemma 3.2 (Policy Gradient Theorem - Applied)

Proof. We adapt the standard policy gradient theorem to our factorized policy structure.

Standard Policy Gradient Theorem The standard policy gradient theorem (Sutton et al., 1999b) states that for a policy π_{θ} and expected return $J(\theta) = \mathbb{E}_{\tau \sim \pi_{\theta}}[R(\tau)]$:

$$\nabla_{\theta} J(\theta) = \int_{\mathcal{S}} \rho^{\pi}(s) \int_{\mathcal{A}} \nabla_{\theta} \pi(a|s; \theta) \cdot Q^{\pi}(s, a) da ds$$

where $\rho^{\pi}(s)$ is the discounted state visitation measure.

A.3.1 State Visitation Distribution in Our Setting

Define $\rho_t^\pi(s)$ as the probability of visiting state $s = (Q, A, T)$ at step t :

$$\rho_t^\pi(s_t) = \sum_{s_{t-1}} \rho_{t-1}^\pi(s_{t-1}) \cdot \pi_d(\text{RESAMPLE}|s_{t-1}) \cdot \pi_{\text{sample}}(A_t, T_t|s_{t-1})$$

This says: to reach state s_t at time t , we must have been at some state s_{t-1} at time $t-1$, chosen to RESAMPLE, and then sampled (A_t, T_t) .

Discounted state visitation:

$$\rho^\pi(s) = \sum_{t=1}^{\infty} \gamma^t \rho_t^\pi(s)$$

At each state $s_k = (Q, A_k, T_k)$, there are two types of actions:

- Sampling actions $a' = (A, T)$ drawn from $\pi_{\text{sample}}(\cdot|s_{k-1})$
- Decision actions $a'' \in \{\text{STOP, RESAMPLE}\}$ drawn from $\pi_d(\cdot|s_k)$

However, these occur at different points in the trajectory:

- After state s_{k-1} , we take sampling action $a'_k = (A_k, T_k)$ to reach state s_k
- At state s_k , we take decision action $a''_k \in \{\text{STOP, RESAMPLE}\}$

For sampling actions at state s_{k-1} :

$$\int_{A_{\text{sample}}} \nabla_\theta \pi_{\text{sample}, \theta}(a'|s_{k-1}) \cdot Q^\pi(s_{k-1}, a') da' = \mathbb{E}_{a' \sim \pi_{\text{sample}}} [\nabla_\theta \log \pi_{\text{sample}, \theta}(a'|s_{k-1}) \cdot Q_{\text{sample}}^\pi(s_{k-1}, a')]$$

For decision actions at state s_k :

$$\sum_{a'' \in \{\text{STOP, RESAMPLE}\}} \nabla_\theta \pi_{d, \theta}(a''|s_k) \cdot Q^\pi(s_k, a'') = \mathbb{E}_{a'' \sim \pi_d} [\nabla_\theta \log \pi_{d, \theta}(a''|s_k) \cdot Q_d^\pi(s_k, a'')]$$

Combining over all states in a trajectory of length T :

$$\begin{aligned} \nabla_\theta J(\theta) &= \mathbb{E}_{\tau \sim \pi_\theta} \left[\sum_{t=1}^T \nabla_\theta \log \pi_{\text{sample}, \theta}(a'_t|s_{t-1}) \cdot Q_{\text{sample}}^\pi(s_{t-1}, a'_t) \right] \\ &\quad + \mathbb{E}_{\tau \sim \pi_\theta} \left[\sum_{t=1}^T \nabla_\theta \log \pi_{d, \theta}(a''_t|s_t) \cdot Q_d^\pi(s_t, a''_t) \right] \end{aligned}$$

We can combine these into a single expectation:

$$\nabla_\theta J(\theta) = \mathbb{E}_{\tau \sim \pi_\theta} \left[\sum_{t=0}^T \left(\nabla_\theta \log \pi_{\text{sample}}(a'_t|s_{t-1}) \cdot Q_{\text{sample}}^\pi(s_{t-1}, a'_t) + \nabla_\theta \log \pi_d(a''_t|s_t) \cdot Q_d^\pi(s_t, a''_t) \right) \right]$$

where we use the convention that terms with $t = 0$ correspond to the initial action. \square

A.4 Proof of Theorem 3.1 (Perfect Attribution of Surrogate Reward)

The surrogate reward for trajectory τ_i is:

$$L_{\text{reward}}(\theta) = \mathbb{E}_{\tau_i \sim \pi_{\text{old}}} \left[\frac{\pi_\theta(\tau_i|Q_i)}{\pi_{\text{old}}(\tau_i|Q_i)} A_i \right]$$

where:

- A_i is the advantage for trajectory τ_i , computed using Group Relative Advantage Estimation (GRAE)
- For query Q_i with multiple sampled trajectories $\{\tau_1, \dots, \tau_G\}$ (the "group"):

$$A_i = \frac{R(\tau_i) - \text{mean}(R(\tau_1), \dots, R(\tau_G))}{\text{std}(R(\tau_1), \dots, R(\tau_G))}$$

- The reward function is $R(\tau) = \mathbb{I}(A_T = A_Q^*)$

Taking the gradient with respect to θ :

$$\nabla_{\theta} L_{\text{reward}}(\theta) = \mathbb{E}_{\tau_i \sim \pi_{\text{old}}} \left[\nabla_{\theta} \left(\frac{\pi_{\theta}(\tau_i | Q_i)}{\pi_{\text{old}}(\tau_i | Q_i)} \right) \cdot A_i \right]$$

Using the log-derivative trick:

$$\nabla_{\theta} \left(\frac{\pi_{\theta}(\tau_i | Q_i)}{\pi_{\text{old}}(\tau_i | Q_i)} \right) = \frac{\pi_{\theta}(\tau_i | Q_i)}{\pi_{\text{old}}(\tau_i | Q_i)} \cdot \nabla_{\theta} \log \pi_{\theta}(\tau_i | Q_i)$$

From Corollary 3.1:

$$\nabla_{\theta} \log \pi_{\theta}(\tau_i | Q_i) = \sum_{k=1}^{T_i} \nabla_{\theta} \log \pi_{\text{sample}, \theta}(A_k, T_k | s_{k-1}) + \sum_{k=0}^{T_i} \nabla_{\theta} \log \pi_{d, \theta}(a_k | s_k)$$

Therefore, when sampling from π_{old} and using importance weighting:

$$\nabla_{\theta} L_{\text{reward}}(\theta) = \mathbb{E}_{\tau_i \sim \pi_{\text{old}}} \left[\frac{\pi_{\theta}(\tau_i | Q_i)}{\pi_{\text{old}}(\tau_i | Q_i)} \cdot A_i \left(\sum_{k=1}^{T_i} \nabla_{\theta} \log \pi_{\text{sample}, \theta}(\cdot) + \sum_{k=0}^{T_i} \nabla_{\theta} \log \pi_{d, \theta}(\cdot) \right) \right]$$

By importance sampling, this equals:

$$\nabla_{\theta} L_{\text{reward}}(\theta) = \mathbb{E}_{\tau_i \sim \pi_{\theta}} \left[A_i \left(\sum_{k=1}^{T_i} \nabla_{\theta} \log \pi_{\text{sample}, \theta}(A_k, T_k | s_{k-1}) + \sum_{k=0}^{T_i} \nabla_{\theta} \log \pi_{d, \theta}(a_k | s_k) \right) \right]$$

Comparing with the policy gradient decomposition from Lemma 3.2, we identify the Q-values by noting that the gradient must have the form:

$$\nabla_{\theta} L_{\text{reward}}(\theta) = \mathbb{E}_{\tau_i \sim \pi_{\theta}} \left[\sum_{k=1}^{T_i} \nabla_{\theta} \log \pi_{\text{sample}, \theta}(\cdot) \cdot Q_{\text{sample}}^{\pi, \text{reward}}(\cdot) + \sum_{k=0}^{T_i} \nabla_{\theta} \log \pi_{d, \theta}(\cdot) \cdot Q_d^{\pi, \text{reward}}(\cdot) \right]$$

For the surrogate reward, both Q-values equal the length-discounted advantage:

$$\begin{aligned} Q_{\text{sample}}^{\pi, \text{reward}}(s_{k-1}, (A_k, T_k)) &= \gamma^{\sum_{j=k}^{T_i} \text{len}(A_j, T_j)} A_i \\ Q_d^{\pi, \text{reward}}(s_k, a_k) &= \gamma^{\sum_{j=k}^{T_i} \text{len}(A_j, T_j)} A_i \end{aligned}$$

Define:

$$\Phi(s_k) = \gamma^{\sum_{j=k}^{T_i} \text{len}(A_j, T_j)} A_i$$

This is the sufficient statistic of future rewards at state s_k . It encodes: "the trajectory will receive advantage A_i at the end, which is at temporal distance $\sum_{j=k}^{T_i} \text{len}(A_j, T_j)$ from now." Then:

$$Q_{\text{sample}}^{\pi, \text{reward}}(s_{k-1}, a'_k) = \Phi(s_k)$$

$$Q_d^{\pi, \text{reward}}(s_k, a''_k) = \Phi(s_k)$$

Both Q-values can be expressed using the same sufficient statistic Φ , evaluated at the appropriate state. This satisfies Definition 3.1 for Balanced Gradient Attribution. \square

A.5 Proof of Theorem 3.2 (Imperfect Attribution of KL Penalty)

We analyze the gradient attribution properties of the token-level KL penalty.

KL Penalty Formulation. The standard token-level KL penalty, computed on trajectories sampled from the current policy, is:

$$D_{KL}^{\text{token}}(\tau) = \sum_{t=1}^{|\tau|} \log \frac{\pi_{\theta}(a_t | s_t)}{\pi_{ref}(a_t | s_t)}$$

where the sum runs over all tokens in trajectory τ . The RL objective includes this as a penalty:

$$J(\theta) = \mathbb{E}_{\tau \sim \pi_{\theta}} \left[R(\tau) - w \cdot D_{KL}^{\text{token}}(\tau) \right]$$

Decomposition Under the Two-Stage Framework. A trajectory τ of length T (i.e., T sampling-decision cycles) consists of:

- T sampling actions, where the k -th sampling action (A_k, T_k) comprises L_k tokens
- T decision actions $a_k \in \{\text{RESAMPLE}, \text{STOP}\}$, each a single token

The total number of tokens is $|\tau| = \sum_{k=1}^T L_k + T$. The KL penalty decomposes as:

$$D_{KL}^{token}(\tau) = \underbrace{\sum_{k=1}^T \sum_{j=1}^{L_k} \log \frac{\pi_{sample,\theta}(token_{k,j} | context)}{\pi_{sample,ref}(token_{k,j} | context)}}_{\text{Sampling component}} + \underbrace{\sum_{k=1}^T \log \frac{\pi_{d,\theta}(a_k | s_k)}{\pi_{d,ref}(a_k | s_k)}}_{\text{Decision component}}$$

Immediate Penalties. Define the immediate KL penalty attributed to each action:

For sampling actions:

$$d_k^{sample} = \sum_{j=1}^{L_k} \log \frac{\pi_{sample,\theta}(token_{k,j} | context)}{\pi_{sample,ref}(token_{k,j} | context)}$$

This is a sum over L_k terms. If individual token-level log-ratios have typical magnitude δ (which may be positive or negative depending on whether the current policy assigns higher or lower probability than the reference), then:

$$|d_k^{sample}| \leq \sum_{j=1}^{L_k} \left| \log \frac{\pi_{sample,\theta}(token_{k,j} | \cdot)}{\pi_{sample,ref}(token_{k,j} | \cdot)} \right| \sim O(L_k \cdot \delta)$$

For decision actions:

$$d_k^{decision} = \log \frac{\pi_{d,\theta}(a_k | s_k)}{\pi_{d,ref}(a_k | s_k)}$$

This is a single scalar:

$$|d_k^{decision}| \sim O(\delta)$$

The ratio of magnitudes is approximately $L_k : 1$. For typical reasoning traces with $L_k \approx 100\text{--}500$ tokens, this represents a two-orders-of-magnitude asymmetry.

Q-Value Recursions.

Proof. The policy gradient for the KL penalty takes the standard form:

$$\nabla_{\theta} \mathbb{E}_{\pi_{\theta}} [D_{KL}^{token}(\tau)] = \mathbb{E}_{\tau \sim \pi_{\theta}} \left[\sum_t \nabla_{\theta} \log \pi_{\theta}(a_t | s_t) \cdot Q^{KL}(s_t, a_t) \right]$$

where $Q^{KL}(s_t, a_t)$ is the expected cumulative KL penalty from taking action a_t at state s_t .

We derive the Q-values by working backwards from the terminal state.

Terminal state (STOP at step T):

$$Q_d^{KL}(s_T, \text{STOP}) = d_T^{decision}$$

There are no future actions, so the Q-value equals the immediate penalty. Magnitude: $O(1)$.

Final sampling action (step T):

$$Q_{sample}^{KL}(s_{T-1}, a'_T) = d_T^{sample} + \gamma \cdot Q_d^{KL}(s_T, \text{STOP})$$

Substituting:

$$Q_{sample}^{KL}(s_{T-1}, a'_T) = d_T^{sample} + \gamma \cdot d_T^{decision} \sim O(L_T) + O(1) \approx O(L_T)$$

The immediate sampling penalty dominates.

Penultimate decision (RESAMPLE at step $T - 1$):

$$Q_d^{KL}(s_{T-1}, \text{RESAMPLE}) = d_{T-1}^{\text{decision}} + \gamma \cdot \mathbb{E}_{\pi_\theta} [Q_{\text{sample}}^{KL}(s_{T-1}, a'_T)]$$

Magnitude:

$$Q_d^{KL}(s_{T-1}, \text{RESAMPLE}) \sim O(1) + \gamma \cdot O(L_T) \approx O(\gamma L_T)$$

The future sampling penalty dominates, but note: the *immediate* contribution is only $O(1)$.

General recursion (for $k < T$):

$$\begin{aligned} Q_{\text{sample}}^{KL}(s_{k-1}, a'_k) &= d_k^{\text{sample}} + \gamma \cdot \mathbb{E}_{\pi_\theta} [Q_d^{KL}(s_k, a''_k)] \\ Q_d^{KL}(s_k, \text{RESAMPLE}) &= d_k^{\text{decision}} + \gamma \cdot \mathbb{E}_{\pi_\theta} [Q_{\text{sample}}^{KL}(s_k, a'_{k+1})] \end{aligned}$$

Scale separation analysis. Define the accumulated future KL from state s_k :

$$V^{KL}(s_k) = \mathbb{E}_{\pi_\theta} \left[\sum_{t \geq k} \gamma^{-t} d_t \mid s_k \right]$$

For the sampling policy at step k :

$$Q_{\text{sample}}^{KL}(s_{k-1}, a'_k) = \underbrace{d_k^{\text{sample}}}_{\sim O(L_k)} + \gamma \cdot V^{KL}(s_k)$$

For the decision policy at step k :

$$Q_d^{KL}(s_k, a''_k) = \underbrace{d_k^{\text{decision}}}_{\sim O(1)} + \gamma \cdot V^{KL}(s_{k+1})$$

Although $V^{KL}(s_k)$ and $V^{KL}(s_{k+1})$ are similar in magnitude (both accumulate future penalties), the *immediate* contributions differ by a factor of L_k .

Impossibility of unified sufficient statistic. Suppose a single sufficient statistic $\Phi : \mathcal{S} \rightarrow \mathbb{R}$ exists such that:

$$\begin{aligned} Q_{\text{sample}}^{KL}(s_{k-1}, a'_k) &= f_{\text{sample}}(s_{k-1}, a'_k, \Phi(s_k)) \\ Q_d^{KL}(s_k, a''_k) &= f_d(s_k, a''_k, \Phi(s_{k+1})) \end{aligned}$$

From the Bellman-style recursions, Φ must satisfy:

$$\begin{aligned} \Phi(s_k) &= O(L_k) + \gamma \Phi(s_{k+1}) \quad (\text{from sampling Q-value}) \\ \Phi(s_k) &= O(1) + \gamma \Phi(s_{k+1}) \quad (\text{from decision Q-value}) \end{aligned}$$

Subtracting: $0 = O(L_k) - O(1)$, which is a contradiction when $L_k \gg 1$.

Therefore, no single sufficient statistic Φ exists. The Q-values require distinct information structures:

$$\begin{aligned} \Phi_{\text{sample}}(s_k) &= d_k^{\text{sample}} + \gamma \Phi_d(s_{k+1}) \sim O(L_k) + \gamma(\cdot) \\ \Phi_d(s_k) &= d_k^{\text{decision}} + \gamma \Phi_{\text{sample}}(s_k) \sim O(1) + \gamma(\cdot) \end{aligned}$$

This establishes Unbalanced Gradient Attribution. □

B Alternative Proof of Theorem 3.1 and Theorem 3.2

The probability of a trajectory τ under the combined policy can be expressed as:

$$P(\tau|Q; \theta) = \left(\prod_{k=1}^T \pi_{sample}(A_k, T_k|s_{k-1}; \theta) \right) \cdot \left(\prod_{k=1}^{T-1} \pi_d(\text{RESAMPLE}|s_k; \theta) \right) \cdot \pi_d(\text{STOP}|s_T; \theta) \quad (1)$$

Taking the logarithm:

$$\log P(\tau|Q; \theta) = \sum_{k=1}^T \log \pi_{sample}(A_k, T_k|s_{k-1}; \theta) + \sum_{k=1}^{T-1} \log \pi_d(\text{RESAMPLE}|s_k; \theta) + \log \pi_d(\text{STOP}|s_T; \theta) \quad (2)$$

Important: The sampling log-probability $\log \pi_{sample}(A_k, T_k|s_{k-1})$ decomposes at the token level as:

$$\log \pi_{sample}(A_k, T_k|s_{k-1}) = \sum_{j=1}^{L_k} \log \pi_{sample}(\text{token}_{k,j}|s_{k-1}, \text{token}_{k,1}, \dots, \text{token}_{k,j-1}) \quad (3)$$

This is a sum of L_k terms—there is no multiplicative $\log(\text{len})$ factor.

The gradient with respect to θ :

$$\nabla_{\theta} \log P(\tau|Q; \theta) = \sum_{k=1}^T \nabla_{\theta} \log \pi_{sample}(A_k, T_k|s_{k-1}; \theta) + \sum_{k=1}^{T-1} \nabla_{\theta} \log \pi_d(\text{RESAMPLE}|s_k; \theta) + \nabla_{\theta} \log \pi_d(\text{STOP}|s_T; \theta) \quad (4)$$

For convenience, we denote $A_0, T_0 = \emptyset$.

B.1 Policy Gradient Decomposition

Using the policy gradient theorem adapted to our factorized policy structure (see Appendix A.3):

$$\nabla_{\theta} J(\theta) = \mathbb{E}_{\tau \sim \pi_{\theta}} \left[\sum_{t=0}^T \left(\nabla_{\theta} \log \pi_{sample, \theta}(a'_t|s_t) \cdot Q^{\pi}(s_t, a'_t) + \nabla_{\theta} \log \pi_{d, \theta}(a''_t|s_t) \cdot Q^{\pi}(s_t, a''_t) \right) \right] \quad (5)$$

B.2 Attribution Analysis for Surrogate Reward

Surrogate Reward Term.

$$L_{clip}(\theta) = \mathbb{E}_{\tau_i \sim \pi_{old}} \left[\frac{\pi_{\theta}(\tau_i|Q_i)}{\pi_{old}(\tau_i|Q_i)} A_i \right] \quad (6)$$

where A_i is the group-relative advantage computed via GRAE:

$$A_i = \frac{R(\tau_i) - \text{mean}(R(\tau_1), \dots, R(\tau_G))}{\text{std}(R(\tau_1), \dots, R(\tau_G))} \quad (7)$$

The probability ratio factorizes as:

$$\frac{\pi_{\theta}(\tau_i|Q_i)}{\pi_{old}(\tau_i|Q_i)} = \underbrace{\left(\prod_{k=1}^{T_i} \frac{\pi_{\theta, sample}(A_k, T_k|s_{k-1})}{\pi_{old, sample}(A_k, T_k|s_{k-1})} \right)}_{\text{Sampling ratio}} \cdot \underbrace{\left(\prod_{k=1}^{T_i-1} \frac{\pi_{\theta, d}(\text{RESAMPLE}|s_k)}{\pi_{old, d}(\text{RESAMPLE}|s_k)} \right)}_{\text{Resampling ratio}} \cdot \underbrace{\frac{\pi_{\theta, d}(\text{STOP}|s_{T_i})}{\pi_{old, d}(\text{STOP}|s_{T_i})}}_{\text{Stopping ratio}} \quad (8)$$

Neglecting the clipping for analytical tractability, the gradient is:

$$\nabla_{\theta} L_{reward} \propto A_i \left[\sum_{k=1}^{T_i} \nabla_{\theta} \log \pi_{\theta, sample}(a'_k|s_{k-1}) + \sum_{k=0}^{T_i} \nabla_{\theta} \log \pi_{\theta, d}(a''_k|s_k) \right] \quad (9)$$

Perfect attribution: The advantage A_i multiplies both sampling and decision gradients equally. Both Q-values reduce to the same sufficient statistic:

$$Q_d^{reward} = Q_{sample}^{reward} \sim \gamma^{\sum_{j=0}^{T_i-k} \text{len}(A_{k+j}, T_{k+j})} A_i \quad (10)$$

B.3 Attribution Analysis for KL Penalty

Token-Level KL Decomposition. The KL penalty decomposes at the token level:

$$D_{KL}^{token}(\tau_i) = \sum_{k=1}^{T_i} \underbrace{\sum_{j=1}^{L_k} \log \frac{\pi_{sample,\theta}(token_{k,j}|\cdot)}{\pi_{sample,ref}(token_{k,j}|\cdot)}}_{d_k^{sample}} + \sum_{k=1}^{T_i} \underbrace{\log \frac{\pi_{d,\theta}(a_k|s_k)}{\pi_{d,ref}(a_k|s_k)}}_{d_k^{decision}} \quad (11)$$

The immediate penalties are:

- **Sampling:** $d_k^{sample} = \sum_{j=1}^{L_k} \log(\pi_\theta / \pi_{ref})$ is a sum of L_k terms $\Rightarrow O(L_k)$
- **Decision:** $d_k^{decision} = \log(\pi_\theta / \pi_{ref})$ is a single term $\Rightarrow O(1)$

Q-Value Recursions. Working backwards from the terminal state:

Value of final STOP action:

$$Q_d^{KL}(s_{T_i}, \text{STOP}) = d_{T_i}^{decision} \sim O(1) \quad (12)$$

Value of preceding sampling action:

$$Q_{sample}^{KL}(s_{T_i-1}, a'_{T_i}) = d_{T_i}^{sample} + \gamma \cdot Q_d^{KL}(s_{T_i}, \text{STOP}) \sim O(L_{T_i}) + O(1) \approx O(L_{T_i}) \quad (13)$$

Value of RESAMPLE action:

$$Q_d^{KL}(s_k, \text{RESAMPLE}) = d_k^{decision} + \gamma \cdot \mathbb{E}_{\pi_\theta}[Q_{sample}^{KL}(s_{k+1}, a'_{k+1})] \sim O(1) + O(\gamma L_{k+1}) \quad (14)$$

Asymmetric Gradient Attribution. The gradient contributions are:

$$\text{Sampling: } \sum_{k=1}^{T_i} \nabla_\theta \log \pi_{sample,\theta}(a'_k|s_{k-1}) \cdot Q_{sample}^{KL}(s_{k-1}, a'_k) \quad (15)$$

$$\text{Decision: } \sum_{k=1}^{T_i} \nabla_\theta \log \pi_{d,\theta}(a''_k|s_k) \cdot Q_d^{KL}(s_k, a''_k) \quad (16)$$

The Q-values have incompatible sufficient statistics:

- Q_{sample}^{KL} : dominated by immediate $O(L_k)$ penalty
- Q_d^{KL} : immediate penalty is $O(1)$, accumulates future sampling penalties

This structural asymmetry arising from the sum over L_k tokens in sampling versus single-token decisions creates **Unbalanced Gradient Attribution**.

C Numerical Illustration of Gradient Attribution

To make the theoretical derivations in the preceding sections concrete, this section presents a simplified numerical example focused on a key scenario: where correct and incorrect answers have the same length. The objective is to trace the flow of gradients from the two primary components of the Group Relative Policy Optimization (GRPO) objective—the surrogate reward¹⁵ and the KL penalty—back to the parameters of the sampling policy (π_{sample}) and the decision policy (π_d).

This exercise will quantitatively demonstrate that the asymmetric regularization effect is not dependent on incorrect answers being more verbose. Instead, it is an architectural consequence of the length-weighted formulation of the KL penalty, which applies a significant penalty to any long generated sequence from π_{sample} while applying a negligible penalty to the single-step actions of π_d .

C.1 Scenario and Policy Parameterization

We establish a minimal yet illustrative scenario to examine the gradient dynamics under the condition of equal answer lengths.

Problem Setup The model is tasked with a simple arithmetic problem: "What is $7 * 8$?".

Action Space

- **Sampling Policy (π_{sample}):** Generates an answer. We consider two outcomes: a Correct answer (C), "56", or a Wrong answer (W), "54".
- **Decision Policy (π_d):** Evaluates the generated answer and chooses to STOP or RESAMPLE.

Policy Parameterization Each policy choice is modeled using a logistic sigmoid function, $\sigma(x) = 1/(1 + e^{-x})$, applied to a single learnable logit (θ).

- **Sampling Policy (π_{sample}):** Governed by a single parameter, θ_s . The probability of generating a correct answer is $P(C|\theta_s) = \sigma(\theta_s)$. We initialize $\theta_s = 0.4$, yielding $P(C) \approx 0.5987$ and $P(W) = 1 - P(C) \approx 0.4013$.
- **Decision Policy (π_d):** Conditioned on the answer from π_{sample} .
 - For a correct answer, the stop probability is $P(\text{STOP}|C, \theta_{d,C}) = \sigma(\theta_{d,C})$. We initialize $\theta_{d,C} = 2.2$, yielding $P(\text{STOP}|C) \approx 0.9002$.
 - For a wrong answer, the resample probability is $P(\text{RESAMPLE}|W, \theta_{d,W}) = \sigma(\theta_{d,W})$. We initialize $\theta_{d,W} = 1.4$, yielding $P(\text{RESAMPLE}|W) \approx 0.8022$.

Length Assignment This is the critical modification for this example. We set the lengths of both correct and incorrect answers to be equal and significant.

- Length of Correct answer: $\text{len}(C) = 8$ tokens.
- Length of Wrong answer: $\text{len}(W) = 8$ tokens.

Reference Policy (π_{orig}) The KL penalty regularizes the current policy (π_θ) against a reference policy (π_{orig}), typically the initial SFT model.

- $\theta_{s,orig} = 0.3 \implies P_{orig}(C) \approx 0.5744, P_{orig}(W) \approx 0.4256$.
- $\theta_{d,C,orig} = 2.0 \implies P_{orig}(\text{STOP}|C) \approx 0.8808$.
- $\theta_{d,W,orig} = 1.2 \implies P_{orig}(\text{RESAMPLE}|W) \approx 0.7685$.

Part 1: Symmetric Gradient Push from the Surrogate Reward

First, we analyze the gradient from the surrogate reward. This calculation is entirely independent of sequence length, demonstrating its symmetric nature.

¹⁵We also simplify the clipped part away

Trajectory and Advantage We consider a single successful trajectory τ_i : the model initially generates a Wrong answer, correctly chooses to RESAMPLE, then generates a Correct answer and correctly chooses to STOP. GRPO is a "critic-less" algorithm that estimates advantage relative to a group of trajectories. We assume this trajectory is better than the group average and assign it a normalized advantage of $A_i = +0.5$.

Gradient Calculation The gradient of the reward objective is $\nabla_{\theta} J_{Reward}(\theta) = A_i \cdot \nabla_{\theta} \log P(\tau_i | \theta)$. The log-probability of the trajectory is: The gradient for each parameter is calculated as follows:

- **For θ_s (Sampling Policy):**

$$\begin{aligned}\nabla_{\theta_s} J_{Reward} &= A_i \cdot \\ &= 0.5 \cdot [-\sigma(\theta_s) + (1 - \sigma(\theta_s))] = 0.5 \cdot [-0.5987 + 0.4013] = \mathbf{-0.0987}\end{aligned}$$

- **For $\theta_{d,W}$ (Decision Policy):**

$$\begin{aligned}\nabla_{\theta_{d,W}} J_{Reward} &= A_i \cdot \nabla_{\theta_{d,W}} \log P(\text{RESAMPLE} | W, \theta_{d,W}) \\ &= 0.5 \cdot (1 - \sigma(\theta_{d,W})) = 0.5 \cdot (1 - 0.8022) = \mathbf{+0.0989}\end{aligned}$$

- **For $\theta_{d,C}$ (Decision Policy):**

$$\begin{aligned}\nabla_{\theta_{d,C}} J_{Reward} &= A_i \cdot \nabla_{\theta_{d,C}} \log P(\text{STOP} | C, \theta_{d,C}) \\ &= 0.5 \cdot (1 - \sigma(\theta_{d,C})) = 0.5 \cdot (1 - 0.9002) = \mathbf{+0.0499}\end{aligned}$$

The advantage A_i is applied as a scalar multiplier to all responsible parameters. The resulting gradients are of a similar order of magnitude, demonstrating a *symmetric push* for improvement.

Part 2: Asymmetric Gradient Drag from the KL Penalty

Next, we analyze the gradient from the KL penalty. The asymmetry arises because the immediate penalty for a sampling action is explicitly weighted by its length, whereas the penalty for a decision action is not.

Calculating KL Penalties and Q-Values We first calculate the immediate KL penalty (d_k) for each step in our trajectory. This measures the "information loss" when the current policy deviates from the reference policy.

- **Step 1 - Sample W:** $d_1^{sample} = 8 \cdot (-\log \frac{0.4013}{0.4256}) = 8 \cdot (0.0588) \approx +0.4704$
- **Step 1 - Resample:** $d_1^{decision} = -\log \frac{0.8022}{0.7685} \approx -0.0429$
- **Step 2 - Sample C:** $d_2^{sample} = 8 \cdot (-\log \frac{0.5987}{0.5744}) = 8 \cdot (-0.0415) \approx -0.3320$
- **Step 2 - Stop:** $d_2^{decision} = -\log \frac{0.9002}{0.8808} \approx -0.0218$

Next, we compute the state-action values ($Q^{\pi, KL}$) by working backward from the end of the trajectory (with discount factor $\gamma = 1$).

- **Value of final action (STOP):** $Q_{KL}(s_2, \text{STOP}) = d_2^{decision} = -0.0218$
- **Value of preceding action (Sample C):** $Q_{KL}(s_1, \text{sample } C) = d_2^{sample} + Q_{KL}(s_2, \text{STOP}) = -0.3320 - 0.0218 = -0.3538$
- **Value of preceding action (RESAMPLE):** $Q_{KL}(s_1, \text{RESAMPLE}) = d_1^{decision} + Q_{KL}(s_1, \text{sample } C) = -0.0429 - 0.3538 = -0.3967$
- **Value of first action (Sample W):** $Q_{KL}(s_0, \text{sample } W) = d_1^{sample} + Q_{KL}(s_1, \text{RESAMPLE}) = 0.4704 - 0.3967 = +0.0737$

Gradient Calculation The gradient of the KL penalty objective is proportional to $\sum_t \nabla_\theta \log \pi_t \cdot Q_{KL,t}$. This gradient acts as a "drag" force, pulling the policy back toward the reference.

- For θ_s (Sampling Policy):

$$\begin{aligned}\nabla_{\theta_s} J_{KL} &\propto \nabla_{\theta_s} \log P(W|\theta_s) \cdot Q_{KL}(s_0, W) + \nabla_{\theta_s} \log P(C|\theta_s) \cdot Q_{KL}(s_1, C) \\ &\propto (-\sigma(\theta_s)) \cdot (0.0737) + (1 - \sigma(\theta_s)) \cdot (-0.3538) \\ &\propto (-0.5987) \cdot (0.0737) + (0.4013) \cdot (-0.3538) = -0.0441 - 0.1420 = \mathbf{-0.1861}\end{aligned}$$

- For $\theta_{d,W}$ (Decision Policy):

$$\begin{aligned}\nabla_{\theta_{d,W}} J_{KL} &\propto \nabla_{\theta_{d,W}} \log P(\text{RESAMPLE}|W) \cdot Q_{KL}(s_1, \text{RESAMPLE}) \\ &\propto (1 - \sigma(\theta_{d,W})) \cdot (-0.3967) = (0.1978) \cdot (-0.3967) = \mathbf{-0.0785}\end{aligned}$$

- For $\theta_{d,C}$ (Decision Policy):

$$\begin{aligned}\nabla_{\theta_{d,C}} J_{KL} &\propto \nabla_{\theta_{d,C}} \log P(\text{STOP}|C) \cdot Q_{KL}(s_2, \text{STOP}) \\ &\propto (1 - \sigma(\theta_{d,C})) \cdot (-0.0218) = (0.0998) \cdot (-0.0218) = \mathbf{-0.0022}\end{aligned}$$

The results are starkly different from the reward gradients. The gradient magnitude for the sampling policy, $|\nabla_{\theta_s} J_{KL}| \approx 0.186$, is more than double that for the first decision parameter ($|\nabla_{\theta_{d,W}} J_{KL}| \approx 0.079$) and over 80 times larger than for the second ($|\nabla_{\theta_{d,C}} J_{KL}| \approx 0.002$). This is the *asymmetric drag*.

Table 3: Breakdown of KL Penalty Gradient Attribution

Step	Action	d_k (Penalty)	$V_{KL}(s')$ (Future)	Q_{KL} (Total)	$\nabla_\theta \log \pi$	Parameter	Contribution
2	STOP	-0.0218	0	-0.0218	$1 - \sigma(\theta_{d,C}) = 0.0998$	$\theta_{d,C}$	-0.0022
2	Sample C	-0.3320	-0.0218	-0.3538	$1 - \sigma(\theta_s) = 0.4013$	θ_s	-0.1420
1	RESAMPLE	-0.0429	-0.3538	-0.3967	$1 - \sigma(\theta_{d,W}) = 0.1978$	$\theta_{d,W}$	-0.0785
1	Sample W	+0.4704	-0.3967	+0.0737	$-\sigma(\theta_s) = -0.5987$	θ_s	-0.0441

C.2 Synthesis: The Net Parameter Update

The final update to the policy parameters is the sum of the gradients from the surrogate reward (the "push") and the KL penalty (the "drag").

Table 4: Summary of Gradient Attribution and Net Update

Parameter	Policy	Reward (Push)	KL (Drag)	Net Gradient	Interpretation
θ_s	π_{sample}	-0.0987	-0.1861	-0.2848	Heavily regularized; stable.
$\theta_{d,W}$	π_d	+0.0989	-0.0785	+0.0204	Learning signal overcomes drag.
$\theta_{d,C}$	π_d	+0.0499	-0.0022	+0.0477	Learning driven by reward.

D Gradient Attribution Properties of SFT and DFT

We analyze the gradient attribution properties of Supervised Fine-Tuning (SFT) and Dynamic Fine-Tuning (DFT) within our two-stage decision-sampling framework. We show that SFT exhibits Unbalanced Gradient Attribution due to policy-entangled Q-values, while DFT removes this entanglement, achieving improved (though not perfect) gradient attribution.

D.1 SFT as Policy Gradient with Implicit Reward

Lemma 3. *The SFT gradient is equivalent to a policy gradient with implicit per-token reward:*

$$\nabla_{\theta} \mathcal{L}_{\text{SFT}} = \mathbb{E}_{\tau \sim \mathcal{D}} \left[\sum_{k=1}^T \sum_{j=1}^{L_k} \nabla_{\theta} \log \pi_{\text{sample}}(\text{token}_{k,j} | \cdot) + \sum_{k=1}^T \nabla_{\theta} \log \pi_d(a_k | s_k) \right] \quad (17)$$

where the implicit reward at each token is $r_t = 1$, but weighted by $1/\pi_{\theta}$ in the gradient (since $\nabla_{\theta} \log \pi = \frac{1}{\pi} \nabla_{\theta} \pi$).

D.2 SFT: Unbalanced Gradient Attribution via Policy-Entanglement

Theorem D.1 (SFT has Unbalanced Gradient Attribution). *For SFT, the implicit Q-values are:*

$$Q_{\text{sample}}^{\text{SFT}}(s_{k-1}, \text{token}_{k,j}) = \underbrace{\sum_{j'=j+1}^{L_k} \frac{1}{\pi_{\text{sample}}(\text{token}_{k,j'})}}_{\text{remaining tokens in step } k} + \underbrace{\frac{1}{\pi_d(a_k | s_k)}}_{\text{decision at step } k} + \underbrace{\sum_{k'=k+1}^T \left(\sum_{j'=1}^{L_{k'}} \frac{1}{\pi_{\text{sample}}(\text{token}_{k',j'})} + \frac{1}{\pi_d(a_{k'} | s_{k'})} \right)}_{\text{future steps}} \quad (18)$$

$$Q_d^{\text{SFT}}(s_k, a_k) = \sum_{k'=k+1}^T \left(\sum_{j'=1}^{L_{k'}} \frac{1}{\pi_{\text{sample}}(\text{token}_{k',j'})} + \frac{1}{\pi_d(a_{k'} | s_{k'})} \right) \quad (19)$$

These Q-values exhibit **policy-entanglement**:

- $Q_{\text{sample}}^{\text{SFT}}$ depends on π_d through the $1/\pi_d(a_k | s_k)$ and $1/\pi_d(a_{k'} | s_{k'})$ terms.
- Q_d^{SFT} depends on π_{sample} through the $1/\pi_{\text{sample}}(\text{token}_{k',j'})$ terms.

Proof. The SFT gradient can be written in policy gradient form:

$$\nabla_{\theta} \mathcal{L}_{\text{SFT}} = \sum_t \nabla_{\theta} \log \pi_{\theta}(a_t | s_t) \cdot Q^{\text{SFT}}(s_t, a_t) \quad (20)$$

where $Q^{\text{SFT}}(s_t, a_t)$ represents the "future value" from taking action a_t at state s_t . Since each token contributes gradient $\nabla_{\theta} \log \pi = \nabla_{\theta} \pi / \pi$, the implicit reward is effectively $1/\pi$ weighted. Working backwards from the terminal state:

At the final decision (STOP at step T):

$$Q_d^{\text{SFT}}(s_T, \text{STOP}) = 0 \quad (21)$$

At the final sampling step T , token j :

$$Q_{\text{sample}}^{\text{SFT}}(s_{T-1}, \text{token}_{T,j}) = \sum_{j'=j+1}^{L_T} \frac{1}{\pi_{\text{sample}}(\text{token}_{T,j'})} + \frac{1}{\pi_d(\text{STOP} | s_T)} \quad (22)$$

Recursively, for step $k < T$:

$$Q_d^{\text{SFT}}(s_k, \text{RESAMPLE}) = Q_{\text{sample}}^{\text{SFT}}(s_k, \text{token}_{k+1,1}) \quad (23)$$

$$Q_{\text{sample}}^{\text{SFT}}(s_{k-1}, \text{token}_{k,j}) = \sum_{j'=j+1}^{L_k} \frac{1}{\pi_{\text{sample}}(\text{token}_{k,j'})} + \frac{1}{\pi_d(a_k | s_k)} + Q_d^{\text{SFT}}(s_k, a_k) \quad (24)$$

The policy-entanglement is evident: $Q_{\text{sample}}^{\text{SFT}}$ contains $1/\pi_d$ terms, and Q_d^{SFT} contains $1/\pi_{\text{sample}}$ terms through the recursive dependency. These Q-values change as π_{θ} updates during training, preventing clean credit assignment. \square

Corollary 2. *No unified sufficient statistic Φ exists for SFT. Following the logic of Theorem 3.2, define:*

$$\Phi_{\text{sample}}^{\text{SFT}}(s_k) = f\left(\frac{1}{\pi_{\text{sample}}}, \frac{1}{\pi_d}, L\right) \quad (25)$$

$$\Phi_d^{\text{SFT}}(s_k) = g\left(\frac{1}{\pi_{\text{sample}}}, \frac{1}{\pi_d}, L\right) \quad (26)$$

Both depend on the full policy π_θ , making $\Phi_{\text{sample}}^{\text{SFT}} \neq \Phi_d^{\text{SFT}}$ in general.

D.3 DFT: Removing Policy-Entanglement

Dynamic Fine-Tuning rescales each token's contribution by its probability:

$$\mathcal{L}_{\text{DFT}}(\theta) = \mathbb{E}_{\tau \sim \mathcal{D}} \left[\sum_{k=1}^T \sum_{j=1}^{L_k} \pi_{\text{sample}}(\text{token}_{k,j}) \cdot \log \pi_{\text{sample}}(\text{token}_{k,j}) + \sum_{k=1}^T \pi_d(a_k | s_k) \cdot \log \pi_d(a_k | s_k) \right] \quad (27)$$

Lemma 4 (Cancellation of $1/\pi$ weighting). *The DFT gradient satisfies:*

$$\pi \cdot \nabla_\theta \log \pi = \pi \cdot \frac{\nabla_\theta \pi}{\pi} = \nabla_\theta \pi \quad (28)$$

Therefore:

$$\nabla_\theta \mathcal{L}_{\text{DFT}} = \mathbb{E}_{\tau \sim \mathcal{D}} \left[\sum_{k=1}^T \sum_{j=1}^{L_k} \nabla_\theta \pi_{\text{sample}}(\text{token}_{k,j}) + \sum_{k=1}^T \nabla_\theta \pi_d(a_k | s_k) \right] \quad (29)$$

The $1/\pi$ weighting is exactly cancelled.

Theorem D.2 (DFT Removes Policy-Entanglement). *For DFT, the implicit Q-values become policy-independent:*

$$Q_{\text{sample}}^{\text{DFT}}(s_{k-1}, \text{token}_{k,j}) = (L_k - j) \cdot c + c + \sum_{k'=k+1}^T (L_{k'} + 1) \cdot c \quad (30)$$

$$Q_d^{\text{DFT}}(s_k, a_k) = \sum_{k'=k+1}^T (L_{k'} + 1) \cdot c \quad (31)$$

where c is a constant independent of π_θ .

Proof. With the $1/\pi$ weighting cancelled, each token contributes constant implicit reward c . Working backwards:

At the final decision:

$$Q_d^{\text{DFT}}(s_T, \text{STOP}) = 0 \quad (32)$$

At step T , token j :

$$Q_{\text{sample}}^{\text{DFT}}(s_{T-1}, \text{token}_{T,j}) = (L_T - j) \cdot c + c \quad (33)$$

where $(L_T - j) \cdot c$ accounts for remaining sampling tokens and c accounts for the final decision. Recursively, for step $k < T$:

$$Q_d^{\text{DFT}}(s_k, \text{RESAMPLE}) = L_{k+1} \cdot c + c + Q_d^{\text{DFT}}(s_{k+1}, a_{k+1}) \quad (34)$$

Expanding the recursion:

$$Q_d^{\text{DFT}}(s_k, a_k) = \sum_{k'=k+1}^T L_{k'} \cdot c + (T - k) \cdot c = \sum_{k'=k+1}^T (L_{k'} + 1) \cdot c \quad (35)$$

Crucially:

- $Q_{\text{sample}}^{\text{DFT}}$ does not depend on π_d .
- Q_d^{DFT} does not depend on π_{sample} .

The Q-values are now policy-independent. \square

D.4 DFT: Remaining Length Asymmetry

Although DFT removes policy-entanglement, length asymmetry persists:

$$Q_d^{\text{DFT}}(s_k, a_k) = c \cdot \sum_{k'=k+1}^T (L_{k'} + 1) \approx c \cdot \sum_{k'=k+1}^T L_{k'} \quad (36)$$

Since $L_{k'} \gg 1$ (sampling sequences contain hundreds of tokens while decisions are single tokens), we have:

$$Q_d^{\text{DFT}} \sim O\left(\sum_{k'} L_{k'}\right) \gg Q_{\text{sample, per-token}}^{\text{DFT}} \sim O(1) \quad (37)$$

The decision policy gradient is weighted by accumulated future sequence lengths, even though each decision is a single token. This creates asymmetric regularization similar to (but weaker than) the KL penalty analyzed in Theorem 3.2.

Property	SFT	DFT	RL (Surrogate Reward)
Q_d depends on π_{sample}	Yes (via $1/\pi_{\text{sample}}$)	No	No
Q_{sample} depends on π_d	Yes (via $1/\pi_d$)	No	No
Q_d depends on future lengths $L_{k'}$	Yes (weighted by $1/\pi$)	Yes (constant weight)	No
Sufficient statistic	$\Phi_{\text{sample}}^{\text{SFT}} \neq \Phi_d^{\text{SFT}}$	$\Phi_{\text{sample}}^{\text{DFT}} \neq \Phi_d^{\text{DFT}}$	$\Phi = \gamma^{\sum \text{len} A_i}$ (unified)
Gradient attribution	Imperfect	Improved	Perfect

Table 5: Comparison of gradient attribution properties.

E Task Description and Experiment Hyperparameters

E.1 Task Description

We evaluate models on multi-digit multiplication tasks, denoted as $m \times n$ where m and n indicate the number of digits in each operand. For example, a 3×4 task involves multiplying a 3-digit number by a 4-digit number (e.g., 123×4567).

Each problem is presented to the model as a natural language query:

Calculate [operand1] * [operand2]. Think step by step.

An answer is scored as correct if and only if the final numerical output exactly matches the ground truth product. Intermediate reasoning steps are not evaluated for correctness.

E.2 Dataset Construction

Training Data. We construct 20,000 training examples for the in-distribution tasks (4×5 and 5×4 multiplication). Operands are sampled uniformly at random within the specified digit range: for an m -digit operand, we sample integers from $[10^{m-1}, 10^m - 1]$. The training set is balanced equally between 4×5 and 5×4 tasks.

Test Data. For each difficulty level (3×3 through 3×9), we construct a test set of 100 examples using the same uniform sampling procedure. No filtering or balancing is applied for the results reported in Table 1. For the calibration analysis in Figure 2, we exclude samples that exceed the 8,192 token generation limit.

SFT Data Variants. We construct two SFT training sets:

- **SFT (no reflection):** Each example consists of a query paired with a chain-of-thought solution leading directly to the answer, without retry patterns.
- **SFT (reflection):** Each example consists of a query paired with a trajectory that may include multiple attempts, explicit error detection, and correction steps before arriving at the final answer.

Trajectory generation procedures are provided in the replication repository.

E.3 Model and Training Details

All experiments use Qwen2.5-7B-Instruct (Qwen et al., 2025) as the base model.

SFT Training. Supervised fine-tuning is conducted using LLaMA-Factory (Zheng et al., 2024). Hyperparameters are as follows:

Hyperparameter	Value
Optimizer	Adam
Batch size	128
Learning rate	1×10^{-5}
Epochs	4.0
Training examples	20,000

Table 6: SFT training hyperparameters.

RL Training. Reinforcement learning is conducted using VeRL (Sheng et al., 2024) with Group Relative Policy Optimization (GRPO). Hyperparameters are as follows:

Hyperparameter	Value
Algorithm	GRPO
Learning rate	1×10^{-6}
Train batch size	512
PPO mini-batch size	128
Rollouts per query (n)	8
KL loss coefficient	0.001
KL loss type	low_var_kl
Max prompt length	1,024 tokens
Max response length	8,192 tokens
Total epochs	2
Gradient checkpointing	Enabled

Table 7: RL training hyperparameters.

E.4 Evaluation Protocol

All models are evaluated with the following settings:

- **Sampling temperature:** 1.0
- **Number of attempts:** 1 (single generation per query)
- **Accuracy metric:** $\frac{\text{Number of correct answers}}{\text{Total number of questions}}$

Confidence Intervals. Confidence intervals for observed accuracy in Table 1 are computed using the normal approximation to the binomial distribution at the 95% level. Confidence intervals for predicted accuracy in Figure 2 are obtained via bootstrapping: we resample the test set with replacement 100 times, compute the predicted accuracy for each bootstrap sample using the calibrated p_s , $p_{d|C}$, and $p_{d|W}$ parameters, and report the 2.5th and 97.5th percentiles of the resulting distribution.

E.5 Compute Resources

Each experiment is conducted on a cloud server equipped with a single NVIDIA H100 GPU.